Fraunhofer Institut
Techno- und
Wirtschaftsmathematik

K.-H. Küfer, M. Monz, A. Scherrer, P. Süss, F. Alonso,
A. S. A. Sultan, Th. Bortfeld, D. Craft, Chr. Thieke

Multicriteria optimization in intensity modulated radiotherapy planning

Berichte des Fraunhofer ITWM, Nr. 77 (2005)

© Fraunhofer-Institut für Techno- und Wirtschaftsmathematik ITWM 2005

ISSN 1434-9973

Bericht 77 (2005)

Alle Rechte vorbehalten. Ohne ausdrückliche, schriftliche Genehmigung des Herausgebers ist es nicht gestattet, das Buch oder Teile daraus in irgendeiner Form durch Fotokopie, Mikrofilm oder andere Verfahren zu reproduzieren oder in eine für Maschinen, insbesondere Datenverarbeitungsanlagen, verwendbare Sprache zu übertragen. Dasselbe gilt für das Recht der öffentlichen Wiedergabe.

Warennamen werden ohne Gewährleistung der freien Verwendbarkeit benutzt.

Die Veröffentlichungen in der Berichtsreihe des Fraunhofer ITWM können bezogen werden über:

Fraunhofer-Institut für Techno- und
Wirtschaftsmathematik ITWM
Gottlieb-Daimler-Straße, Geb. 49

67663 Kaiserslautern
Germany

Telefon: +49 (0) 6 31/2 05-32 42
Telefax: +49 (0) 6 31/2 05-41 39
E-Mail: info@itwm.fraunhofer.de
Internet: www.itwm.fraunhofer.de

Vorwort

Das Tätigkeitsfeld des Fraunhofer Instituts für Techno- und Wirtschaftsmathematik ITWM umfasst anwendungsnahe Grundlagenforschung, angewandte Forschung sowie Beratung und kundenspezifische Lösungen auf allen Gebieten, die für Techno- und Wirtschaftsmathematik bedeutsam sind.

In der Reihe »Berichte des Fraunhofer ITWM« soll die Arbeit des Instituts kontinuierlich einer interessierten Öffentlichkeit in Industrie, Wirtschaft und Wissenschaft vorgestellt werden. Durch die enge Verzahnung mit dem Fachbereich Mathematik der Universität Kaiserslautern sowie durch zahlreiche Kooperationen mit internationalen Institutionen und Hochschulen in den Bereichen Ausbildung und Forschung ist ein großes Potenzial für Forschungsberichte vorhanden. In die Berichtreihe sollen sowohl hervorragende Diplom- und Projektarbeiten und Dissertationen als auch Forschungsberichte der Institutsmitarbeiter und Institutsgäste zu aktuellen Fragen der Techno- und Wirtschaftsmathematik aufgenommen werden.

Darüberhinaus bietet die Reihe ein Forum für die Berichterstattung über die zahlreichen Kooperationsprojekte des Instituts mit Partnern aus Industrie und Wirtschaft.

Berichterstattung heißt hier Dokumentation darüber, wie aktuelle Ergebnisse aus mathematischer Forschungs- und Entwicklungsarbeit in industrielle Anwendungen und Softwareprodukte transferiert werden, und wie umgekehrt Probleme der Praxis neue interessante mathematische Fragestellungen generieren.

Prof. Dr. Dieter Prätzel-Wolters
Institutsleiter

Kaiserslautern, im Juni 2001

Multicriteria optimization in intensity modulated radiotherapy planning

Karl-Heinz Küfer[1], Michael Monz[1], Alexander Scherrer[1],
Philipp Süss[1], Fernando Alonso[1], Ahmad Saher Azizi Sultan[1],
Thomas Bortfeld[2], David Craft[2], Christian Thieke[3]

1: Department of Optimization,*
Fraunhofer Institut for Industrial Mathematics (ITWM),
Gottlieb-Daimler-Straße 49, 67663 Kaiserslautern, Germany
E-mail: *kuefer,monz,scherrer,suess,alonso,sultan@itwm.fhg.de*

2: Department of Radiation Oncology,*
Massachusetts General Hospital and Harvard Medical School,
30 Fruit Street, Boston, MA 02114, USA
E-mail: *tbortfeld,dcraft@partners.org*

3: Clinical Cooperation Unit Radiation Oncology,
German Cancer Research Center (DKFZ),
Im Neuenheimer Feld 280, 69120 Heidelberg, Germany
E-mail: *c.thieke@dkfz-heidelberg.de*

*work partially supported by NIH grant CA103904-01A1

Abstract

Inverse treatment planning of intensity modulated radiothrapy is a multicriteria optimization problem: planners have to find optimal compromises between a sufficiently high dose in tumor tissue that garantuee a high tumor control, and, dangerous overdosing of critical structures, in order to avoid high normal tissue complcication problems.

The approach presented in this work demonstrates how to state a flexible generic multicriteria model of the IMRT planning problem and how to produce clinically highly relevant Pareto-solutions. The model is imbedded in a principal concept of *Reverse Engineering*, a general optimization paradigm for design problems. Relevant parts of the Pareto-set are approximated by using *extreme compromises* as cornerstone solutions, a concept that is always feasible if box constraints for objective funtions are available. A major practical drawback of generic multicriteria concepts trying to compute or approximate parts of the Pareto-set is the high computational effort. This problem can be overcome by exploitation of an inherent *asymmetry* of the IMRT planning problem and an adaptive approximation scheme for optimal solutions based on an adaptive clustering preprocessing technique. Finally, a coherent approach for calculating and selecting solutions in a real-timeinteractive decision-making process is presented. The paper is concluded with clinical examples and a discussion of ongoing research topics.

Keywords: multicriteria optimization, extreme solutions, real-time decision making, adaptive approximation schemes, clustering methods, IMRT planning, reverse engineering

1 The IMRT treatment planning problem

Radiotherapy is, besides surgery, the most important treatment option in clinical oncology. It is used with both curative and palliative intention, either solely or in combination with surgery and chemotherapy. The vast majority of all radiotherapy patients is treated with high energetic photon beams. Hereby, the radiation is produced by a linear accelerator and delivered to the patient by several beams coming from different directions (see figure 1).

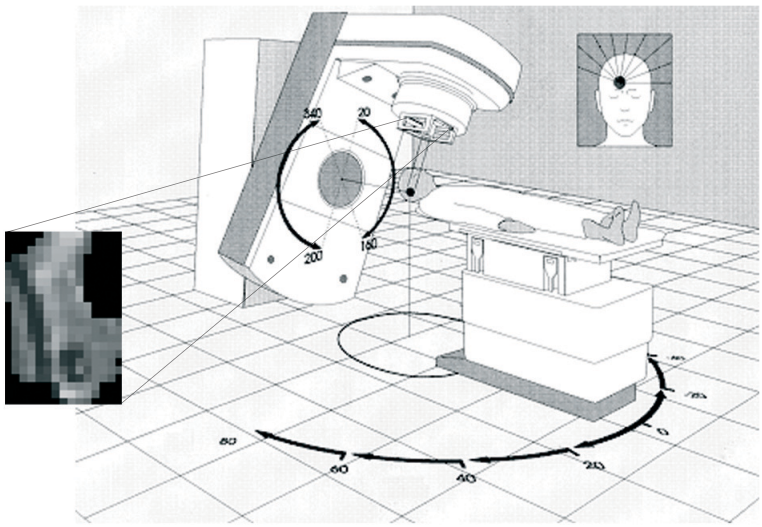

Figure 1: The gantry can move around the couch on which the patient lies and the couch itself may be moved to alter the directions

In conventional conformal radiation therapy, only the outer shape of each beam can be smoothly adapted to the individual target volume. The intensity of the radiation throughout the beams cross section is uniform or only coarsely modified by the use of pre-fabricated wedge filters. This, however, limits the possibilities to fit the shape of the resulting dose distribution in the tissue to the shape of the tumor, especially in the case of irregularly shaped non-convex targets like paraspinal tumors.
This limitation is overcome by *intensity-modulated radiation therapy* (IMRT) [44]. Using multi-leaf collimators (MLCs) (see figure 2), the intensity is modulated by uncovering parts of the beam only for individually chosen opening times (monitor units) and covering the rest of the beam opening by the collimator leafs. This allows for a more precise therapy by tightly conforming

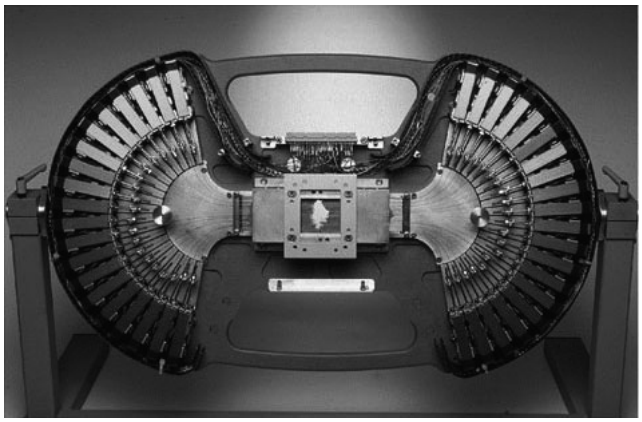

Figure 2: A Multileaf Collimator (MLC). The square opening in the centre of the machine is partially covered by leafs, each of which can be individually moved. (picture from: [38])

the high dose area to the tumor volume. The optimization approaches described here are designed originally for IMRT planning, but are applicable to conventional planning and intensity-modulated *proton* therapy (IMPT) as well, because no assumptions on the physics of the delivery is made in the modeling.

An IMRT treatment plan is physically characterized by the beam arrangement given by the angle of the couch relative to the gantry and the rotation angle of the gantry itself, and by the intensity modulation of each beam (see figure 1). The treatment aim is to deliver sufficient radiation to the tumor while sparing as much of the healthy tissue as possible. Finding ideal balances between these inherently contradictory goals challenges dosimetrists and physicians in their daily practice.

The *treatment planning problem* is to find an optimal set of parameters describing the patient treatment. While the choice of a particular delivery scheme (radiation modality, energies, fractionation, etc.) is by far not a trivial decision to make, it will be considered given in our context. These decisions are made based on clinical expertise and do not lend themselves to a mathematical programming approach. The number of beams and their directions relative to the patient (*setup geometry*) and the intensity distribution of the beams (*fluence maps*), on the other hand, may be subjected to optimization routines.

Finding an optimal setup geometry and an optimal set of intensity maps using a global optimization model ([8], [22]) has the disadvantage that the resulting problem is highly non-convex, as the following example demonstrates. Assume the target is given by the rectangular shape in the middle

of figure 3, and the smaller rectangular structures at the corners of the target are critical volumes.

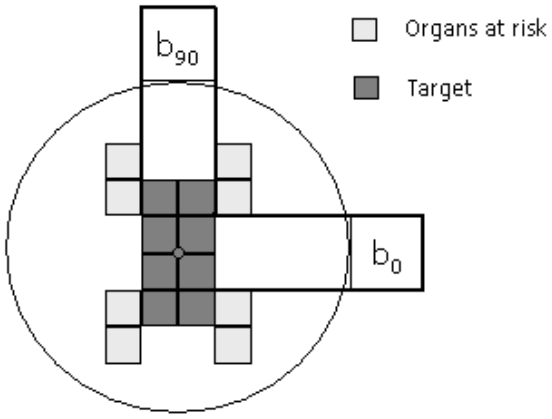

Figure 3: Optimization of the setup geometry is highly nonconvex

The beams may be arranged anywhere on the depicted circle. Then the optimal beam direction is given by beam b_{90}. A search for this optimum may, however, get stuck in a local minimum like beam b_0. Notice that the search would have to make a very big change in the current solution to leave this local optimum. Any global problem formulation is therefore difficult to solve, and cannot be done reasonably fast. If heuristics are used to solve the problem, there are no guaranties for the optimality of the solution.
On the other hand, a very detailed search on the potential beam positions is in many cases not necessary. If the critical part of the body is covered by the beams' irradiation, the optimization of the intensity maps will mitigate the errors due to non-optimal beam directions substantially. However, in some cases like head-and-neck treatments, computer-based setup optimization might be of considerable value. Brahme [7] mentions some techniques useful to handle setups with only a few beams.

Aside from the resulting dose distribution, the complexness of the beam geometry also has to be considered when evaluating the quality of a treatment plan. In most cases (see e.g. [5], [4], [7] or [14]), an *isocentric* model is used for the choice of the setup geometry, i.e., the central rays of the irradiation beams meet in one single point, the *isocenter of irradiation* (see figure 4).
To further facilitate an automated treatment delivery, usually also a coplanar beam setting is used. Then the treatment can be delivered completely by just rotating the gantry around the patient without the need to rotate or translate the treatment couch between different beams. This leads to shorter overall treatment times which are desirable both for stressing the patient as little as possible and for minimizing the treatment costs. Beam geometry

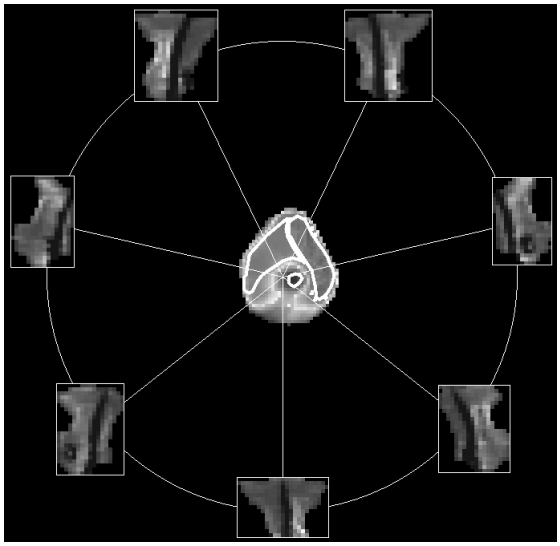

Figure 4: Fluence maps for different beam directions intersecting at the tumor

optimization is still an interesting problem in its own right and it needs to be addressed. However, in this paper we will not discuss any such solution approaches but merely assume that the irradiation geometry is given.

In the conventional approach to solve the treatment planning problem, "forward treatment planning" has been the method of choice. The parameters that characterize a plan are set manually by the planner, and then the dose distribution in the patient is calculated by the computer. If the result was not satisfactory, the plan parameters are changed again manually, and the process starts over. As the possibilities of radiotherapy become more sophisticated (namely with intensity modulation), Webb argues [43] that "it becomes quite impossible to create treatment plans by forward treatment planning because:

- there are just too many possibilities to explore and not enough human time to do this task
- there is little chance of arriving at the optimum treatment plan by trial-and-error
- if an acceptable plan could be found, there is no guaranty it is the best, nor any criteria to specify its precision in relation to an optimum plan."

Furthermore, there is no unified understanding of what constitutes an optimum treatment plan, since the possibilities and limitations of treatment

planning are case-specific and might even change during the planning process.

Therapy planning problems have in the last two decades been modeled using an *inverse* or *backward* strategy (see e.g the survey paper [7]): given desired dose bounds, parameters for the treatment setup are found using computerized models of computation.

The approach to work on the problem from a reverse angle, i.e. from a description of a desired solution to a configuration of parameters that characterizes it, is an established approach in product design called *reverse engineering*.

2 Optimization as a reverse engineering process

Reverse engineering has been used in various disciplines and there are many ways to interpret its meaning. In software development, for example, the functionality of a program is specified before the first line of code is written. Another typical example of reverse engineering is a company using an envisioned or existing product as a model for development. It is possible to extract the same concept of all formulations of reverse engineering: one of an inverse approach to solving a problem. This means that the solution is obtained from the specification of ideal properties, rather than from a syntactical description of parameters and some recipe.

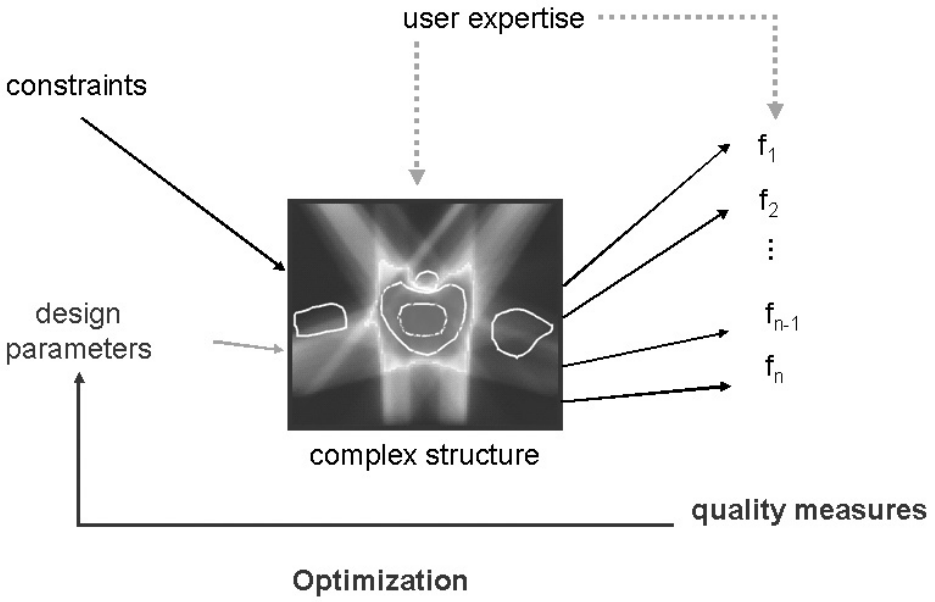

Figure 5: Illustration of the reverse engineering concept

The setting we find in IMRT planning is typical of a large-scale design problem. Refer to figures 5 and 6 for an illustration of the following discussion. In order to maintain an abstract setting here, we will only assume that there exists the need to design a complex structure $\mathbf{d}(\mathbf{x})$ contained in the structure space $\mathbb{D}$ (e.g. a physical product, a treatment plan, a financial portfolio, etc.)

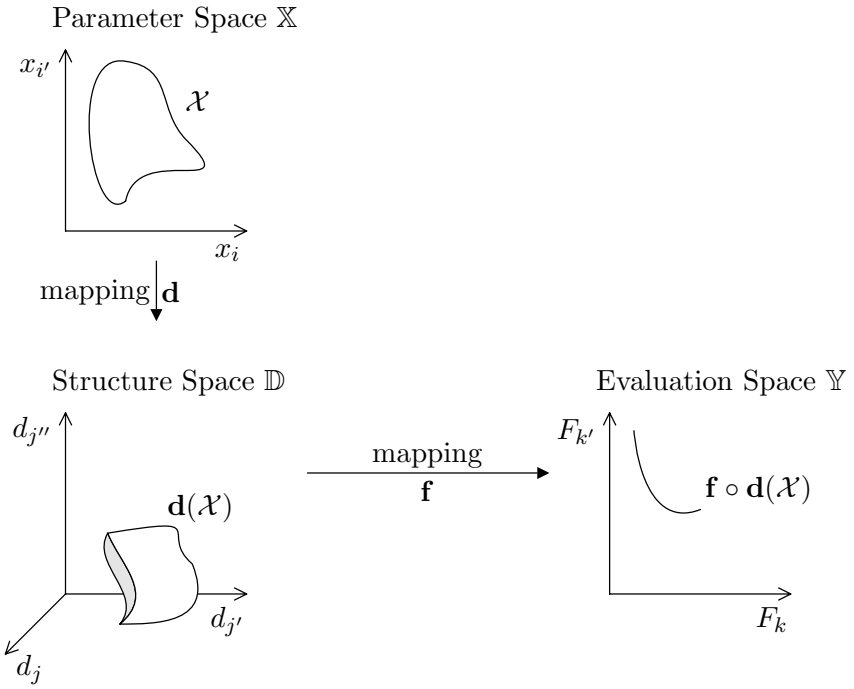

Figure 6: Illustration of the spaces involved in the general design problem

depending on an element $\mathbf{x}$ of the space of parameters $\mathbb{X}$, that fulfills certain design contraints. Given design parameters that distinguish a solution, it can be simulated with the help of a "virtual design tool". This aid possesses the capability to virtually assemble the final solution when given the setup parameters and relevant constraints, effectively evaluating an element of $\mathbb{D}$.

This is done using evaluation functions $f_k : \mathbb{D} \to \mathbb{R}$. The composites $F_k = f_k \circ \mathbf{d}$ of f_k and the mapping $\mathbf{d} : \mathbb{X} \to \mathbb{D}$ are called indicator functions. These, in turn, are used to judge a design.

The main difference to forward engineering is that the reverse approach is a more systematic solution procedure. While the iterations in forward engineering resemble a trial-and-error approach, it is the formal optimization that is characteristic for our reverse engineering concept.

Since a complex structure usually cannot be assigned a single "quality score" accepted by any decision-maker, there are typically several indicator functions $F_k, k \in \mathcal{K}$. Thus, the problem is recognized as a *Multicriteria Opti-*

mization Problem

$$\begin{array}{rcl} \mathbf{F}(\mathbf{x}) & \rightarrow & \min \quad \text{subject to} \\ \mathbf{x} & \in & \mathcal{X}, \end{array} \tag{1}$$

where $\mathbf{F}(\mathbf{x}) = (F_k(\mathbf{x}))_{k \in \mathcal{K}}$.

The quest for a solution that has a single maximal quality score should be transformed to one for solutions that are *Pareto optimal* [13] of *efficient*. A solution satisfying this criterion has the property that none of the individual criteria can be improved while at least maintaining the others. The affirmative description is: if the Pareto optimal solution is improved in one criterion, it will worsen in at least one other criterion.

In general, solutions obtained and selected using a strategy that considers the multicriteria setting of Pareto-optimality explicitly not only allow more freedom in specifying objectives, they also seem in a sense much more "stable" to the decision-maker.

2.1 Stability of solutions in Multicriteria Decision-Making

Consider the following example of selecting a solution from the evaluation space in 2 dimensions (refer to figures 7 and 8). The region is bounded and the arrows indicate the descent directions of the objective functions set by the decision-maker. It is clear that the solutions must lie on the boundary of the feasible region, the *Pareto boundary*.

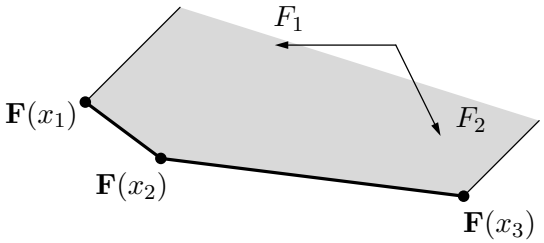

Figure 7: Solution space and given descent directions. The bold boundaries are candidate solutions.

The evaluations of the efficient solutions in our example are indicated by the bold part of the boundary. Notice that if only one criterion is chosen to base a decision on, the objective function will reduce to one of its components F_1 or F_2. In our example, the candidate set reduces to a single solution, namely x_1 if F_1 is chosen and x_3 if F_2 is the selected direction. Depending on the scalarization, any point on the frontier can be achieved. However, optimization methods will typically deliver one of the "corners" as a solution. Also, given the steepness of the frontier in direction from $\mathbf{F}(x_2)$ to $\mathbf{F}(x_3)$, and the directions of the objective functions, it is most likely that either $\mathbf{F}(x_1)$ or $\mathbf{F}(x_2)$ will be the returned solution.

If the decision-maker now alters the objective function to produce similar descent directions with $\tilde{F}_2$ as new objective function (F_1 remains unchanged), the efficient frontier remains the same. However, with the new objective function, it becomes more likely that candidate $\mathbf{F}(x_3)$ will be chosen. Thus, in a scalarized optimization problem, the change in the objective functions could cause a rather big "jump" on the frontier. Communicating the entire

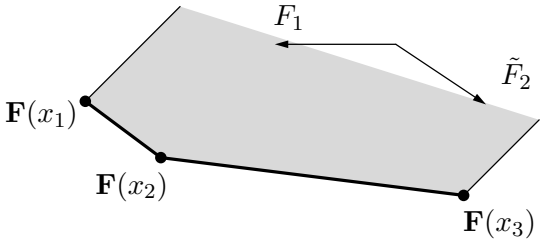

Figure 8: A change in objective functions retains the candidate set.

shape of the frontier, rather than jumping from one solution to the next, results in much more information being conveyed to the user. This also alleviates the effects of only broad specifications of optimization parameters.

Notice that in general it is not possible to avoid the "jumpiness" of single solution by adjusting the parameters of the scalarization. Therefore, a true multicriterial evaluation of the solutions is imperative.

Our discussion on the stability in a true multicriteria decision-making framework can be taken as an argument to relax the requirement to be overly specific in the choice of a particular objective function - a topic of current discussion in the medical physics literature. If alternative indicator functions are in a sense correlated (i.e. an improvement in one leads to an imrpovement in the other), the resulting candidate sets of solutions are rather similar. Since the indicator functions used were deviced to measure the same clinical outcome, it should not be surprising that most of these functions are rather highly correlated. In fact, Romeijn et al. have shown that for a lot of objective functions commonly used in modeling the treatment planning problem, the solutions comprising the Pareto set remain the same [35]. The process of choosing a well-suited candidate according to the preferences of the decision-maker is an interesting topic in itself and addressed in section 5.

2.2 Multicriteria optimization strategies

A realization of the conventional strategies mentioned above is a method we label the "Human Iteration Loop": this is depicted in figure 9. This strategy has several pitfalls that are all avoidable. First, the solutions generated this way will be subject to the sensitivity described above. In addition, the

decision-maker is forced to transform the several objectives into a scalarized objective function - a difficulty we will address in section 3.

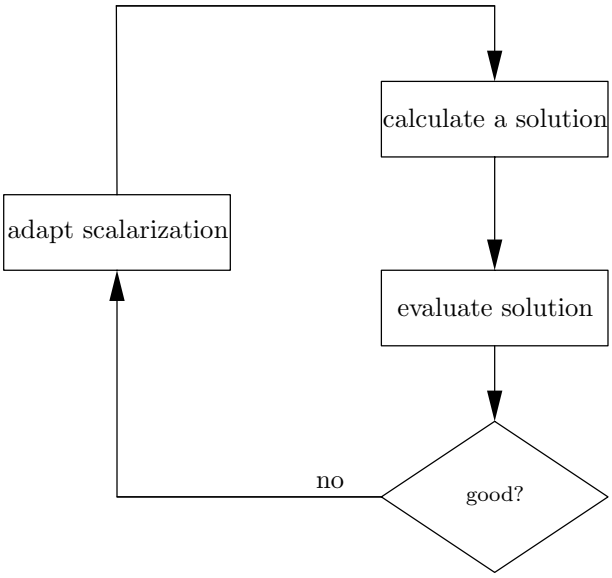

Figure 9: Human iteration loop described as method of *successive improvements*

Given a large dimension of $\mathbb{X}$, it is impossible to ask the decision-maker for optimization parameters that leads to an ideal solution in the first iterate. An iterative adjustment of the parameters converges to a solution that hardly incorporates any wishes that are not explicitly modelled. It is perhaps even presumptuous to expect a decision-maker to specify an ideal solution in terms of the indicator functions exactly, let alone to ask for exact trade-offs between all pairs of objectives. Initial demands on the solution properties might thus very well be reverted when the outcome is seen as a whole. This may be a result of the realization that the initial conviction of an ideal was blemished or simply the realization that the description was not complete. In any case, any model of an ideal that is "cast in stone" and inflexible is detrimental to the design process. A truly multicriterial decision-making framework would allow for flexible modeling because it is able to depict more information and supports the stability in the decision-making process.

Weights in a scalarization approach, for example, are nothing but an attempt to translate the decision-maker's ideal into arbitrary weights. This artificial nature results from having to quantify global trade-off rates between different objectives that are often of very different nature. The fact that no information on efficiency can be conveyed allows only maximum time or a maximum number of repetitions as stopping rules for this process.

These arguments render the Human Iteration Loop a futile effort. Instead, a method that is designed for a multicriteria setting must be installed.

With a large number of objective functions comes a high dimensional boundary and with this a large number of directions to look for potential solutions for our problem. For this reason, there exist methods to attempt to convey the shape of the boundary to the decision-maker. This is most often done implicitly, either by giving the decision maker a myriad of solutions that approximate the boundary, or by interactively calculating representative solutions that are Pareto optimal. Miettinen [26] adopts the following classification of methods to attain practical solutions:

1. **no-preference methods**
   methods where no preference information is used, i.e. methods that work without specification of any optimization parameters

2. **a posteriori methods**
   preference is used a posteriori, i.e. the system generates a set of Pareto optimal solutions of which the decision maker selects one

3. **a priori methods**
   where the decision maker has to specify his preferences through some parameters prior to the calculation and

4. **interactive methods**
   where preferences are not necessarily stated prior to calculations, but are revealed throughout.

The large-scale situation in treatment planning forbids the application of purely interactive methods, and pure a priori methods are not flexible enough for our demands. With a posteriori methods in the strict sense usually comes a complex re-evaluation after the actual optimization, while no-preference methods do not allow any goal-directed planning. We therefore develop in the later chapters a hybrid method that is a combination of an interactive and an a posteriori method. Some information given a priori is used to automatically attain a set of Pareto-optimal points, and a real-time interactive method uses the pre-computed results for the selection of the final solution. In a sense, the methodology described here incorporates advantages of all the methods classified above.

Unlike the Human Iteration Loop, our method does not require the decision-maker to formulate an individual scalarization problem. Rather, after specifying ideal values and bounds, the user will be presented with a database of Pareto-optimal solutions calculated offline, which can be navigated in real-time in a clever way to choose a plan that is in accordance with the preferences of the decision-maker.

In chapter 3, we will describe how the solutions are obtained, and in chapter 5, we will address the issues faced when selecting from a range of solutions. Note that the pre-computation of plans is done without any human interaction, thus taking out the *Human* of the mundane *Iteration Loop*. But even if the user is left out of the optimization, with high dimensions of the spaces involved comes a costly computation of a candidate solution set. Thus, the problems that need to be solved have to be manageable by an optimization routine.

Specifying properties a solution should have, to return to the idea of reverse engineering, implicitly places restrictions on the parameters. As the parameters are not evaluated directly, the mapping $\mathbf{d} : \mathbb{X} \to \mathbb{D}$ necessarily becomes a "subroutine" in the iterations of the optimization process - only a structure can be qualitatively judged in a meaningful way. Many descent algorithms used in optimization evaluate the objective function rather often during run-time, making this subroutine a significant driver for the complexity.

In applications, this often corresponds to time-consuming simulations. In the IMRT case it is the dose mapping, which is a costly calculation if the degree of discretization is rather fine. A method to cope with this computational difficulty has to be established. Typical design problems have a numerical property that, if exploited, makes the many necessary computations of plans possible: asymmetry.

2.3 Asymmetry in linear programming

In a typical design problem the number of parameters is rather small compared to the number of relations describing the structure in terms of the parameters. This arises naturally when the mapping $\mathbf{d} : \mathbb{X} \to \mathbb{D}$ is linear and $dim(\mathbb{X}) \ll dim(\mathbb{D})$. We know from linear programming that, in absence of strong degeneracy, the number of constraints that are binding at an optimal solution is about $dim(\mathbb{X})$, a comparably small number. The other roughly $dim(\mathbb{D}) - dim(\mathbb{X})$ inequalities are not sharp - they play no role in this particular solution. This is common for regions of the structure that play a minor role in the current quality specifications, for example. We call such a situation where a majority of relations are inconsequential to the optimal solution *asymmetric*. Consider the linear problem

$$\begin{aligned} \mathbf{c}^T\mathbf{x} &\to \min \quad \text{subject to} \\ \mathbf{A}\mathbf{x} &\leq \mathbf{b} \end{aligned} \tag{2}$$

where $\mathbf{c} \in \mathbb{X}$ and $\mathbf{A} \in \mathbb{R}^{\dim(\mathbb{D})\times\dim(\mathbb{X})}$ is a matrix with the row vectors $\mathbf{a}_j$, i.e. $\mathbf{d}(\mathbf{x}) = \mathbf{A}\mathbf{x}$.

For a solution $\mathbf{x}^* \in \mathbb{X}$ of this linear problem, a number of the inequalities are fulfilled with equality, i.e. $\mathbf{x}^*$ is located in the intersection of the corresponding hyperplanes $\{\mathbf{x} \in \mathbb{X} : \ \mathbf{a}_j \cdot \mathbf{x} = b_j\}$. The other inequalities are fulfilled with "$<$". This means the linear problem is *asymmetric* in the sense that exact knowledge of the values $\mathbf{a}_j \cdot \mathbf{x}$ is only required for the binding relations, whereas using more or less exact approximations of the other values would not affect the solution $\mathbf{x}^*$. In other words, we could get away with an approximate $\mathbf{A}'$, which is ideally of a much simpler structure and thus allows a faster evaluation of the approximate mapping $\mathbf{d}' : \mathbf{x} \mapsto \mathbf{A}'\mathbf{x}$.

Asymmetry is, in fact, a very common property of large-scale linear programming problems modeling reverse engineering. Optimization techniques have been developed to deal with such situations; the most well known in the linear setting is column generation (in our case *row* generation).

In this approach, briefly, the solution is iteratively improved by a selective scheme - the generation of rows or columns - that alters only a promising part of the current solution. In *Integer Programming*, the method of *cutting planes* successively provides more detailed information about the region that contains an optimal solution. Algorithmically, aggregation-disaggregation techniques [32] provide these refinements. These strategies begin with a coarse description of a solution and refine the details only where they matter most. They usually trade off efficiency for accuracy by selecting an approximation once, solving it, and export the solution to the original problem.

In our case, one also obtains a slim problem formulation that is easier to solve than the original. It will prove successful if a clever disaggregation scheme is found that iteratively refines the aggregated problem formulation so that the optimal solutions converge. The method we suggest may be called *adaptive problem approximation*. This strategy, in short, produces a sequence of optimization problems starting with a very coarse description, and iteratively refines the formulation until the optimal solution to the approximate is also optimal for the original problem.

While all of the aggregation-disaggregation, cutting plane and column generation techniques only adjust and refine parts of the feasible region, the adaptive problem approximation also modifies the objective function. Note that the indicator functions $\mathbf{F}(\mathbf{x})$ are composites of $\mathbf{d}$ and $\mathbf{f}$. Of course, modifying $\mathbf{d}$ also changes $\mathbf{F}$. Therefore, our method not only modifies the solution space, it also simplifies the objective function while still steering the solution towards the optimum of the original problem.

To summarize,

1. conventional treatment planning does not live up to the excpectations of a modern clinical decision-making process,

2. the multicriteria setting can be coped with by appropriate optimization methods and clever schemes for selecting a solution presented in later chapters, and

3. in order to manage the computations, we exploit the asymmetry of the treatment planning problem.

In the following chapter we describe the a posteriori part of the multicriterial framework for the treatment planning problem. The interactive component is subject of section 5. In most cases various criteria and objectives in the target volume(s) and in several critical structures have to be considered. As was mentioned above, this cannot be done with a single scalar objective function.

3 Multicriteria optimization

This chapter is mainly concerned about the techniques used to realize the strategies set out in the previous chapter. Coupled with the ideas from chapter 2 to exploit possible asymmetries of the problem structure, our approach described here is a fast method to calculate a candidate set of Pareto solutions. We need such a candidate set for our decision-making procedure in section 5. The discussion of the methods in this section is, however, not limited to a large-scale or asymmetric situation but also valid for relatively simple general multicriteria optimization problems.

The mathematical discipline to find solutions that are Pareto-optimal is multicriteria optimization ([26], [39]). The theory of multicriteria optimization is mainly focusing on convex problems for the same reason why the field of nonlinear optimization theory focuses much on the same class of problems. A multiobjective optimization problem is convex if all the objective functions and the feasible region are convex. It is for this and only marginally more general classes of problems that we can guaranty optimality in any sense. In a convex setting, a local minimum is also a global optimum and any descent method will deliver such solutions. We will base the following discussion on the assumption that we deal with convex problem descriptions.

For convex problems the set of all Pareto optimal solutions forms a connected part of the boundary of the set of all evaluated solutions [42]. If we take $\mathcal{X}$ to be the set of feasible solutions, then $\mathbf{F}(\mathcal{X})$ is the set of evaluations. The *Pareto boundary* is a connected subset of the boundary of its convex hull $\text{conv}\,(\mathbf{F}(\mathcal{X}))$. The boundary has a dimension of at most $|\mathcal{K}|-1$, where $|\mathcal{K}|$ is the number of objective functions in the problem formulation. It has a lower dimension if some of the functions are independent of the others, resulting in the boundary being "flat" or fully determined in that dimension.

In IMRT, the multicriteria setting stems from the separate evaluations of a dose distribution in the various volumes of interest (VOI). These reveal the trade-offs in changing from one treatment plan to another. There are many examples in which some organs are natural "opponents". In cases of prostate cancer, the rectum and the bladder are such opponents (cf. figure 10). In

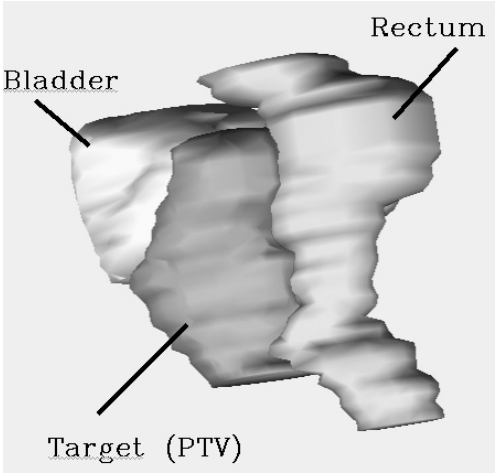

Figure 10: Exemplary prostate case where the target volume is situated between two critical structures

head-neck cases, sparing more of the spinal chord typically means inflicting more damage on the brain stem or the parotid glands. Another example of conflicting goals is the aspired homogeneity of the dose distribution in the target versus the overdosage of some organs at risk. Also, choosing more than one indicator function for a volume not seldom render the problem multicriterial.

Reverse engineering now enters the picture by setting prescribed goals for the indicator functions. This allows any method to begin to look for Pareto optimal treatment plans by guiding the search by given goals. What is needed to create a model are specific evaluation functions.

3.1 Typical evaluation functions

The quality of a treatment plan determined by an intensity vector $\mathbf{x}$ with respect to a clinical structure is modeled by an evaluation function f, that maps the corresponding dose distribution $\mathbf{d}(\mathbf{x})$ to a real value $f(\mathbf{d}(\mathbf{x}))$. For simplification, the critical structures in the body are discretized into small volume parts V_j called *voxels* (more on this in chapter 4). Standard evaluation functions include those that measure deviations from a desired dose value L in the target T:

$$f(\mathbf{d}(\mathbf{x})) = \max_{V_j \subseteq T} |L - d(V_j)(\mathbf{x})|, \tag{3}$$

or functions which penalize voxel doses exceeding an upper bound U in an organ at risk R:

$$f(\mathbf{d}(\mathbf{x})) = \Big(|R|^{-1} \sum_{V_j \subseteq R} \max\left(d(V_j)(\mathbf{x}) - U,\, 0\right)^q \Big)^{\frac{1}{q}}, \quad q \in [1, \infty). \tag{4}$$

where $|R|$ denotes the number of voxels in R. Another choice are functions which take account of the whole shape of a dose distribution by means of an EUD, cf. e.g. [6]. Using for example A. Niemierko's EUD [29], the deviation for the organ at risk R from U is measured by

$$f(\mathbf{d}(\mathbf{x})) = \frac{1}{U} \Big(|R|^{-1} \sum_{V_j \subseteq R} d(V_j)(\mathbf{x})^q \Big)^{\frac{1}{q}}, \quad q \in [1, \infty), \tag{5}$$

The EUD measure for an organ at risk (OAR) is derived by finding the homogeneous dose corresponding to the tumor control probability (TCP) or normal tissue complication probability (NTCP) for OAR in an inhomogeneous dose distribution. Figure 11 illustrates two possible EUD evaluations of a *dose volume histogram* (DVH).
TCP and NTCP are statistical functions that measure the probability of destroying clonogenic cells of the tumor and the probability of damaging risk organs, respectively, dependent on dosages. Lower dose bounds for the target and upper dose bounds for organs that guaranty a high probability of tumor control and a low probability of damaging risks can be derived using these function based on statistics gained from experiences with thousands of treated patients (see, e.g. [11]). These histograms depict the percentage of a VOI that receives at least a certain dose over the relevant dose interval and is depicted by the solid line. The dotted and the dashed lines are EUD measures with q about 1 and q close to ∞, respectively. Thus, the dotted line is equivalent to the original histogram under the EUD-measure using $q = 1$. Organs that work parallel (e.g. lungs, kidneys) are often evaluated using values for q that are close to 1, whereas serial organs such as the spinal chord are evaluated with relatively high values for q.
EUD as an evaluation function is being investigated in many models of current research and seems to be a promising approach [35] because many non-convex criteria can be transformed into convex functions that have equivalent Pareto optimal solutions.

The basic property of the mentioned evaluation functions is convexity and a resulting optimization model can be guarantied to be solved to optimality. The physician may nevertheless evaluate the plan on the basis of non-convex criteria like dose volume histogram constraints.

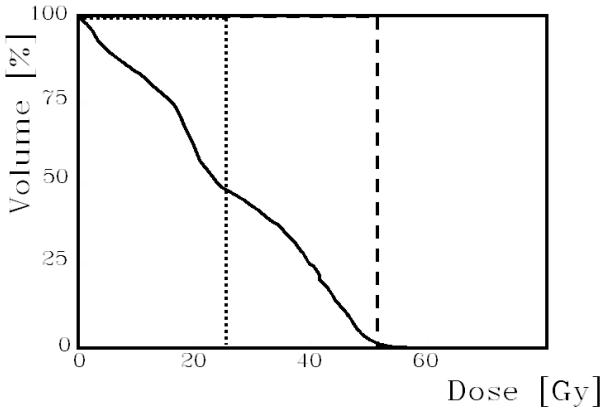

Figure 11: Exemplary DVH curve. The quality of a plan are first judged by the shape of these histograms.

A DVH-constraint reads

$$\mathrm{DVH}_k(d_k^{\max}) \leq V_k^{\max}. \tag{6}$$

In words, dose values greater than $d_k^{\max}$ are allowed in at most $V_k^{\max}$ voxels of the k^{th} structure. It is often acceptable to overdose small parts of a volume to be able to achieve a more favourable distribution in the tumor.
Incorporating DVH constraints into the optimization results in a global non-linear problem with no guaranty for optimality. In [33], Romeijn et al propose a different type of dose-volume constraint: that the *avergage* dose received by a subset of a target receives dose inside a given interval. A constraint formulation of this type results in a piece-wise linear constraint by interpreting it as a well-known conditional Value-at-Risk measure in financial engineering.

3.2 Pareto solutions and the planning domain

Currently, it is common practice to use the weighted sum approach as a model for computations. An initial set of weights is decided and the clinical quality of the solution is checked by eye using appropriate dose visualizations. The weights are adjusted and a new solution is obtained. This is reminiscent of our discussion of the human iteration loop (figure 9, page 11). It is time consuming and does not allow dynamic treatment planning (cf. Bortfeld [5]).

As was mentioned at the beginning of this section, our method is also based on gathering preference information after the calculation of some Pareto

solutions. It is neither possible nor meaningful to calculate all efficient solutions. It is not possible because the Pareto-front is a coherent and therefore an infinite subset of the set of feasible solutions. It is also not meaningful because there are many Pareto solutions that are clinically irrelevant.

For instance, in the example given in Figure 12 one would not go from point A with dose levels of 11 Gy in the spinal cord and 13 Gy in the parotid gland to the upper left efficient solution with dose levels of 9 Gy (spinal cord) and 33 Gy (parotid gland). In other words, the 2 Gy dose reduction

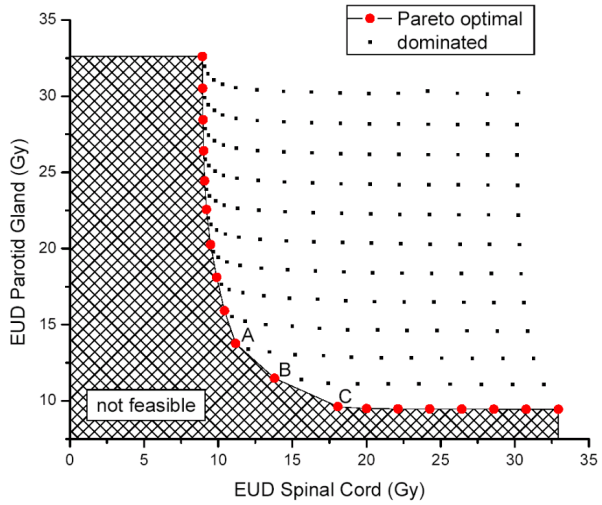

Figure 12: Exploration of the Pareto front for a head and neck case by brute force methods. Every square dot represents one treatment plan. A total of 16x16=256 plans was generated. The round dots represent the Pareto front for this case, i.e., the set of efficient treatment plans.

in the spinal cord at this low dose level is not worth the price of a 20 Gy dose increase in the parotid gland, which may cause xerostomia.
We therefore try to focus on parts of the Pareto boundary that contain clinically meaningful plans. Since it is easier to classify clinical irrelevance than relevance, we try to exclude as many irrelevant plans as possible and call the remaining set of possible plans the *planning domain* $\mathcal{X}_u$.

The first step is to exclude plans that exceed the clinically acceptable values in the indicator functions by introducing hard constraints. These *box constraints* should be set rather generously in order to allow a flexible range of solution outcomes from which experts may select an appropriate candidate. Of course, the more flexible this range is selected to be, the more calculations will be necessary. If chosen too strict, they may, however, lead to infeasibility. This serves as a first indication to the decision-maker that

the initial appraisement of the situation was utopian. After possibly several relaxations of the box constraints, the oncologist may realize that more irradiation directions are needed to find a clinically acceptable solution and alter the geometry accordingly.

A further restriction that improves the clinical relevance of the plans contained in $\mathcal{X}_u$ is a restriction on the trade-off between different indicator functions. This can be incorporated into the model using *ordering cones*. The drawback of using such ordering cones lies in the fact that it is complicated to work with them algorithmically in a nonlinear setting.
Another possibility to ensure bounded trade-off rates is to modify the scalarization functions to ensure that the trade-offs are bounded (for details, cf. [16], [17]).

3.3 Solution strategies

Once a planning domain is fixed, the problem to solve is given by

$$\begin{aligned} \mathbf{F}(\mathbf{x}) &\rightarrow \min \quad \text{subject to} \\ \mathbf{x} &\in \mathcal{X}_u, \end{aligned} \tag{7}$$

where $\mathbf{F}$ is the vector of indicator functions, and $\mathbf{x}$ is a fluence map. Usually multicriteria problems are solved by formulating possibly multiple scalarized versions of the problem. There are several standard methods along with their variations which can be used to solve the multicriteria problem and which exhibit different characteristics.

One possibility is to solve the *lexicographic problem*. It treats the objective functions one by one in a fixed order according to the preference of the decision-maker.

$$\begin{aligned} F_{(1)}(\mathbf{x}), \ldots, F_{(|\mathcal{K}|)}(\mathbf{x}) &\rightarrow \text{lex min} \quad \text{subject to} \\ \mathbf{x} &\in \mathcal{X}_u \end{aligned} \tag{8}$$

The theoretical justification to use the solution of problem (8) requires the decision maker to be able to arrange the objective functions according to their absolute importance. This implies that an indicator function $F_{(m)}$ that was ranked more important than some other criterion $F_{(n)}$, i.e. $m < n$, is infinitely more important to the decision maker [26]. As this assumption cannot be made in clinical practice, this approach is not applicable in this context.

The *weighted sum approach* lets the decision-maker choose weights w_k for a structure $k \in \mathcal{K}$ in the weighted scalarization problem

$$\begin{aligned} F_w(\mathbf{x}) = \sum_{k \in \mathcal{K}} w_k F_k(\mathbf{x}) \quad &\rightarrow \quad \min \quad \text{subject to} \\ \mathbf{x} \quad &\in \quad \mathcal{X}_u. \end{aligned} \tag{9}$$

These weights have no other meaning than to ensure comparability between the objective functions.

Another standard approach is the *ε-constraint* method.

$$\begin{aligned} F_l(\mathbf{x}) \quad &\rightarrow \quad \min \quad \text{subject to} \\ F_j(\mathbf{x}) \quad &\leq \quad \varepsilon_j \text{ for all } j \in \mathcal{K} \\ \mathbf{x} \quad &\in \quad \mathcal{X}_u, \end{aligned} \tag{10}$$

where all $l \in \mathcal{L}$ must be minimized successively to ensure Pareto optimality [26]. The bounds ε are varied to obtain different results. If chosen appropriately, every Pareto optimal plan can be found.
The drawback of the ε-constraint method is that the bounds used during the different scalar optimizations usually form a fine grid whose size grows exponentially in the number of dimensions.

The last approach to be mentioned is the *compromise programming* or the *weighted metric* approach ([26], [48], [51]). Here, a reference point is chosen and the distance to it is minimized in a suitable metric.
The reference point must be outside the feasible region. The ideal point - the point given by the minima of the individual indicator functions - or some utopia point - a point that is smaller than the ideal point in each component - can be used as a reference point.
The different components of $\mathbf{F}(\mathbf{x})$ are scaled to get different solutions. Alternatively, the metric can be varied, or both. The solutions obtained are guarantied to be Pareto optimal if the metric is chosen appropriately and the scaling parameters are positive.

A popular choice is the Tchebycheff problem, even though it does not guaranty to produce Pareto optimal solutions.

$$\begin{aligned} \max_{k \in \mathcal{K}} \{\sigma_k F_k(\mathbf{x})\} \quad &\rightarrow \quad \min \quad \text{subject to} \\ \mathbf{F}(\mathbf{x}) \quad &\leq \quad \mathbf{u} \\ \mathbf{x} \quad &\in \quad \mathcal{X}_u \end{aligned} \tag{11}$$

The choice of the scaling $\boldsymbol{\sigma}$ is difficult for the same reasons why it is difficult to formulate a relevant planning domain: the decision-maker may not know enough about the case a priori.

Note that scaling is not the same as choosing weights for a problem like the weighted scalarization (9) above. The scaling coefficients $\boldsymbol{\sigma}$ contain information about the willingness to deteriorate relative to the specified reference point, while the weights in (9) represent the "global importance" of an indicator function. The scaling can be derived from ideal values for the indicator functions as in [20]. The ideal values are much more natural for a practitioner; they are easier to find than a set of artificial weights or a preference order on the indicators.

Many algorithms in multicriteria optimization identify the Pareto set in the space of parameters [10]. The final decision will be made in terms of the objectives, however. Also, "(s)ince the dimension of $(\mathbf{F}(\mathcal{X}_{\mathrm{Par}}))$ is often significantly smaller than the dimension of $(\mathcal{X}_{\mathrm{Par}})$, and since the structure of $(\mathbf{F}(\mathcal{X}_{\mathrm{Par}}))$ is often much simpler than the structure of $(\mathcal{X}_{\mathrm{Par}})$" [2], we are interested in the distinguishing features of the Pareto boundary in the space of evaluations, the F-space. That is, we want the shape of $\mathbf{F}(\mathcal{X}_{\mathrm{Par}})$, where

$$\mathcal{X}_{\mathrm{Par}} := \{\mathbf{x} \in \mathcal{X}_u \mid \mathbf{x} \text{ is Pareto optimal}\}$$

In order to convey this shape to the user, we need a mechanism to approximate the boundary.

3.4 Approximation of the Pareto boundary

To obtain an initial set of representatives of $\mathcal{X}_{\mathrm{Par}}$ we propose a generalization of the solution obtained by solving problem (11): *extreme compromises*. The extreme compromises balance so-called *active indicator functions* only and Pareto optimality is enforced.

Let $\emptyset \neq \mathcal{M} \subseteq \mathcal{K}$ be the indices of the active indicators. Let $\mathcal{N}_0 := \mathcal{M}$, $\mathbf{u}^{(0)}$ be the bounds of the planning domain and $i = 0$. Then the solution of the following procedure is called extreme compromise for the active indicators $\mathcal{M}$.

1. Solve:

$$\begin{aligned} \max_{j \in \mathcal{N}_i}\{F_j(\mathbf{x})\} &\rightarrow \min \quad \text{subject to} \\ \mathbf{F}(\mathbf{x}) &\leq \mathbf{u}^{(i)} \\ \mathbf{x} &\in \mathcal{X}_u \end{aligned} \tag{12}$$

2. Let $\mathbf{y}^{(i)}$ be the optimal objective value of the above optimization problem and $\mathcal{O}_i \subseteq \mathcal{N}_i$ be the subset of indicators that cannot be further improved. Then let

$$\begin{aligned} \mathbf{u}_j^{(i+1)} &:= \mathbf{y}^{(i)} \text{ for } j \in \mathcal{N}_i, \\ \mathcal{N}_{i+1} &:= \mathcal{N}_i \setminus \mathcal{O}_i \text{ and} \\ i &:= i + 1 \end{aligned}$$

3. If $\mathcal{N}_i \neq \emptyset$, goto 1.

4. Repeat the above procedure with $\mathcal{N}_{i+1} := \mathcal{K} \setminus \mathcal{M}$, $\mathbf{u}^{(i+1)} := \mathbf{u}^{(i)}$ and $i := i + 1$.

The approach is a kind of mixture between weighted metric and lexicographic optimization. The solution for $\mathcal{M} = \mathcal{K}$ is also a solution of the Tchebycheff problem (11). It can easily be shown, that the extreme compromises are Pareto optimal.

With this setting, we will find therapy plans that give an equibalanced solution for active indicator functions $F_k \in \mathcal{M}$, while the remaining non-active functions with indices $k \in \mathcal{N}$ satisfy the relaxed condition of staying in $\mathcal{X}_{\text{Par}}$. The rationale behind the definition of the extreme compromises is to fathom the possibilities for simultaneously minimizing groups of organs for all possible choices of grouping them.

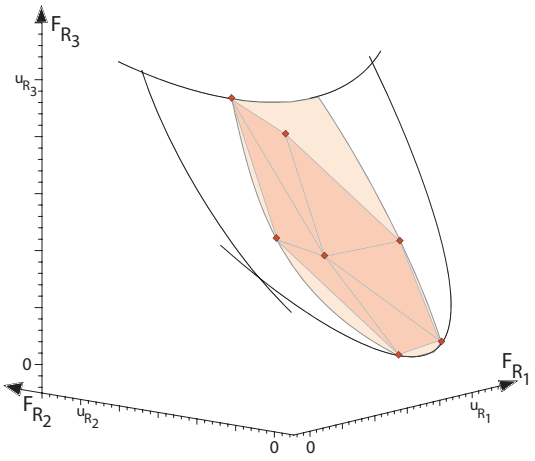

Figure 13: Extreme compromises in 3 dimensions. The solution in the "center" is the equibalanced solution. Starting from the solution obtaining the highest value in F_{R_3} and rotating clock-wise, the solutions are obtained by minimizing (i) $\{F_{R_1}\}$, (ii) $\{F_{R_1}, F_{R_2}\}$, (iii) $\{F_{R_2}, F_{R_3}\}$, (iv) $\{F_{R_2}\}$, (v) $\{F_{R_3}\}$, (vi) $\{F_{R_1}, F_{R_3}\}$. The larger of the shaded regions is the planning domain. The shaded region contained in the planning domain is the convex hull of the extreme compromises - the part of the front that is of interest to us.

The extreme compromises are typically not of high clinical relevance, but they mark a relatively large region within $\mathcal{X}_{\text{Par}}$ in which the interesting solutions are contained.
The complexity of such a generation of extreme compromises is exponential, as the number of optimization problems of type (12) is $2^{|\mathcal{K}|-1}$ in terms of the

number of evaluation criteria (because the empty set of indicator functions needs no optimization).
Of course, the exponential number of problems of type (12) we have to solve is a result of the high dimension of the Pareto boundary we are interested in and is thus to some extend problem inherent.
One method to reduce the number of computations is to group related organs and treat them as one component. They are turned active or inactive as a group and hence only count as one indicator in the exponential complexity term. In a head and neck case one could for example group the eyes with their respective optical nerve since it most often does not make sense to spare one while applying critical doses to the other.

It is a common observation that typically not more than 5 organs or organ groups are critical in finding the desired compromise. Hence, if we knew these *tradeoff-entities* afore, the indicators for all other entities can be disregarded as active indicators in (12) thus reducing the amount drastically.
As it was mentioned in chapter 2, these calculations are technical and done without any human interaction, so the calculations could for example run over night.

If we want to convey the continuous set $\mathbf{F}(\mathcal{X}_{\text{Par}})$ to the planner, we need a good approximation of it. Using a fine discrete approximation induces an unbearable computational load for higher dimensions since the number of solutions needed is most probably of the order of

$$O\left((1/\rho)^{dim(\mathbf{F}(\mathcal{X}_{\text{Par}}))}\right),$$

where ρ is the grid width. In words, the number of calculations needed to guaranty a grid where the distance between the points is at most ρ is proportional to the above complexity measure. Furthermore, as $\mathbf{F}(\mathcal{X}_{\text{Par}})$ is not known a priori the solutions will not be evenly spread on the Pareto boundary and hence there will be a lot of solutions whose distance is much smaller than ρ. Thus, asking for a very fine discrete approximation is neither recommendable for computational reasons, nor is it sensible in practice, as solutions lying very close together on the boundary do not differ enough to warrant separate investigation.

To overcome the above characterized dilemma, we use *interpolation* to fill the gaps in between the Pareto optimal solutions as a continuous approximation of the Pareto boundary. Figure 14 shows a convex combination between two solutions in 2 dimensions. The resulting F-vector is shown as well. As can be seen, this plan is in all likelihood not Pareto optimal, and we will address this issue in chapter 5.
Since the continuous approximation using convex combination does not care for large gaps as long as the interpolates stay close to the Pareto boundary the quality measure for the approximation is different. Due to convexity the

interpolated solution is at least as good as the interpolated **F**-vectors of the interpolation partners (figure 14). Thus, if the distance between the convex hull of the indicator function values and the Pareto boundary is small so is the distance for the interpolated plans. Note though, that using just the extreme compromises, the approximation attained by the spanned region will contain notably suboptimal points.
A method that fits well to this quality measure are of the class of *Normal Boundary Intersection* techniques (cf. Das [9]). Here, briefly, the additional points are found by refining an initially crude approximation of the boundary given by the convex hull of the indicator's individual minima. The maximum distance from this hull to the boundary is found and a new Pareto solution is added there.

As it is, all deterministic methods to approximate a boundary use a triangulation scheme or convex hull as subprocedures to organize or find the optimization parameters. So does the Normal Boundary Intersection and thus the idea is, as many techniques proposed, sound for low dimensions but, unfortunately, computationally infeasible for higher dimensions. Even the space it would take to manage the number of simplices in the triangulation would exceed all reasonable bounds.

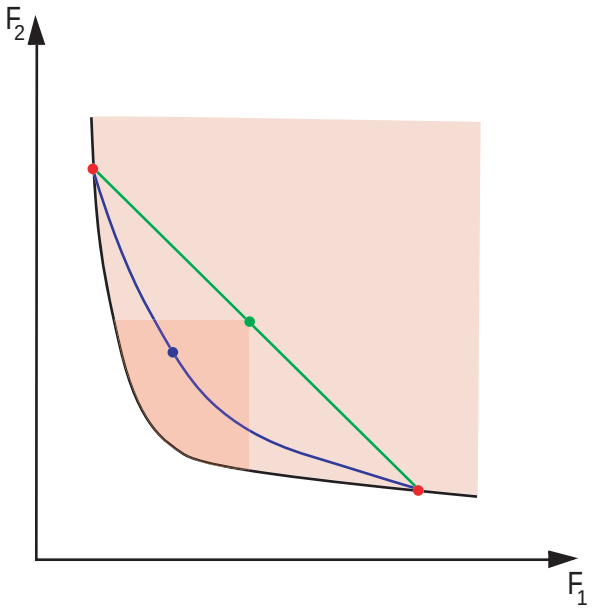

Figure 14: The interpolation of the F-vectors of two interpolated solution is in general worse than the F-vector of the interpolate

The *curse of dimensions* can only be overcome in realistic time by some stochastic procedure that fills gaps in the approximation. In many approxi-

mation problems if the dimension exceeds a certain threshold the stochastic procedures even yield better results in expectation.
For the stochastic procedure the scaling in a weighted metric problem similar to problem (11) is chosen randomly from a uniform distribution. It is so far an open question whether it is worthwhile to use non-uniform distributions which make it less likely that a new parameter set is chosen that is close to an already used one. The distribution of the solutions in the non-uniform case would clearly be better, but to update the distribution after the calculation of a solution and the evaluation of the distribution needs additional computational effort that could thwart the effect of the improved distribution.

4 The numerical realization

4.1 Aspects of discretization

The width of the leaf channels of the MLC used to apply the treatment implies natural slices of each beam. In case of the static plan application ('step and shoot method'), typically, these slices are dissected into quadratic *beamlets* B_i whose edge length is identical to the width of the leaf channel, on

Figure 15: Schematic form of an intensity map

which the intensity map attains constant values, see figure 15, and can thus be representated by a vector $\mathbf{x} = (x(B_i))$. The discretization on the beams in case of the dynamic plan application ('sliding window method') may be a different one, which does not alter the form of the discrete representation. The discretization in the volume is typically based on small cuboid-shaped *voxels* V_j, in which the dose distribution is assumed to be locally constant. Their size is usually related to the distance between adjacent CT-slices, i.e. the edge lengths correspond to this distance. The dose distribution can thus be representated by a vector $\mathbf{d} = (d(V_j))$. As there are typically up to a few thousand beamlets and the several hundred thousand voxels, we are dealing with a truly large scale optimization problem.

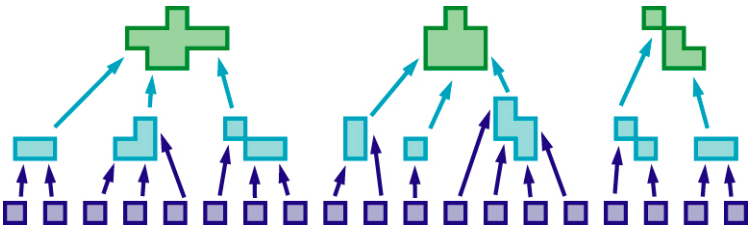

Figure 16: Schematic discretization of volumes.

As a consequence of the superposition principle of dose computation for photons (see figure 4), the dose distribution for an intensity vector then follows as

$$\begin{aligned} \mathbf{d} : \mathbb{X} &\rightarrow \mathbb{D}, \\ \mathbf{x} &\mapsto \mathbf{P} \cdot \mathbf{x}, \end{aligned}$$

with $\mathbf{P}$ being the *dose-information* matrix. The entry p_{ji} of the dose-information matrix represents the contribution of beamlet B_j to the absorbed dose in voxel V_i under unit intensity, depending on modality and energy spectrum of the radiation used. Hence, the dose $\mathbf{d}(V_j)$ in voxel V_j depends on the row vector $\mathbf{p}(V_j) = (p_{ji})_i$. There are several methods to attainthese values: they might be calculated using the pencil beam approach, a superposition algorithm, or some Monte Carlo method. In this paper we do not discuss this important issue; we assume $\mathbf{P}$ to be given in some satisfactory way.

4.2 The adaptive clustering method

Plan quality is measured by evaluating a dose distribution in the involved clinical structures. Typically, during plan optimization the dose distribution will attain an acceptable shape in most of the volume, such that the final quality of a treatment plan strongly depends on the distribution in some small volume parts, where e.g. the descent of radiation from the cancerous to the healthy structures implies undesirable dose-volume effects.
Based on this problem characteristic, several approaches to reduce the computational complexity of the problem by manipulations in the volume have been tried (cf. the listing in [49]). These manipulations are done by heuristic means in advance of the optimization routine and incorporate e.g. the use of large voxels in less critical volume parts, a restriction to the voxels located in pre-defined regions of interest or a physically motivated selection of voxels. However, such heuristic problem modifications will possibly lead to an insufficient control on the dose distribution during the optimization and a thus uncontrollably worsened plan quality.

The *adaptive clustering method* overcomes these defects by an individual adaptation in the volume. We provide a small example in 4.3. This was introduced in [20] and it is discussed in detail in [37]. We will only briefly explain it here.
In a preprocessing step, the original dose-volume information is successively aggregated to *clusters* consisting of merged voxels with their corresponding dose information, forming a *cluster hierarchy* with different levels. This *hierarchical clustering process* is independent of how dose distributions are evaluated; that is, it is independent of the actual indicator function being used. This corresponds to a simplified dose mapping as mentioned in chapter 2. Figure 17 shows for a clinical head neck case the progress of the hierarchical clustering process in a transversal voxel layer.

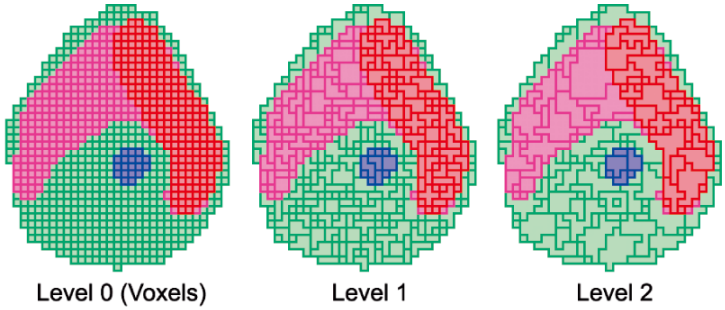

Figure 17: The clusterings of the levels $l = 0, \ldots, 2$ in a transversal voxel layer. In this layer, the boost volume is located on the right side, the target on the left and the spinal cord in the centre. The remainder is unclassified tissue.

Created only once for an IMRT planning problem, the resulting cluster hierarchy will then serve as a 'construction kit' to generate adapted volume discretizations for the subsequent optimization problems. Each such optimization starts on a coarse clustering, that consists of clusters of the upper hierarchy levels. While the optimization runs, the algorithm gradually detects those volume parts responsible for high contributions to the objective function and replaces the corresponding clusters in *local refinement* steps by smaller ones to improve the local control on the dose distribution. Discretizations with clusters from different levels are called *adapted clusterings*. Transversal slices of such adapted clusterings are shown in figure 18.
Due to the individual adaptation of the volume structure during the optimization by the *local refinement process*, the result is an optimum of the original problem, but with a significantly smaller expense than a voxel-based optimization would have required. Numerical experiments on several sets of real clinical data typically show a reduction in computation time by a factor of about 10. Optimization on both structures yield plans with very similar

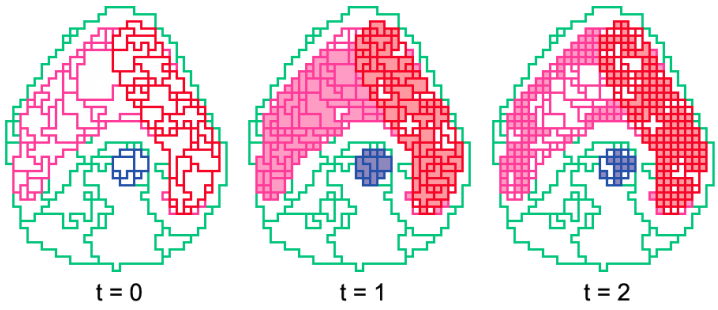

Figure 18: The adapted clusterings for a transversal voxel layer at the beginning of the local refinement process ($t = 0$) and after the first ($t = 1$) and second ($t = 2$) local refinement step. The filled clusters are the ones that were refined in the previous step.

evaluation function values.
This algorithmic concept determines the general architecture of our numerical solver, that consists of a solver kernel surrounded by a numerics shell. The numerics shell performs the refinement steps and provides the solver kernel with the restricted optimization problems based on the adapted clusterings. The kernel approximates each restricted optimization problem by a sequence of nonrestricted problems by an exterior penalty function method [1, 9.2], which are then solved using conjugate direction methods [1, 8.8].

4.3 Asymmetry in the inverse treatment planning problem

The decisively reduced computational expense obtained by the adaptive clustering method traces back to the asymmetry of the inverse treatment planning problem. Consider the treatment planning problem as general design problem, cf. 2.3. The quality of a dose distribution in a volume of interest the planner deems relevant in making a decision is measured by an evaluation function f. We will specify some of these functions in section 3.1. The function measuring the quality of a plan characterized by $\mathbf{x}$ with respect to a volume of interest can thus be considered as a composition $F(\mathbf{x}) = f(\mathbf{P} \cdot \mathbf{x})$ of the dose mapping and the evaluation function.
Consider the simplified problem to apply a high dosage d_T in the tumor, and a small dosage d_{R_k} in a critical volume R_k. That is, the quality functions to be minimized are of the form

$$F_{R_k}(\mathbf{x}) = \max_{V \subseteq R_k} \mathbf{p}(V) \cdot \mathbf{x} - d_{R_k}$$

and

$$F_T(\mathbf{x}) = d_T - \min_{V \subseteq T} \mathbf{p}(V) \cdot \mathbf{x},$$

where $V \subseteq R_k$ and $V \subseteq T$ are the voxels composing the critical volume respectively the tumor, and $\mathbf{p}(V)$ are the corresponding row vectors of $\mathbf{P}$.

To find e.g. an equibalanced solution, cf. 3, we formulate the following linear problem.

$$\begin{aligned} s &\rightarrow \min \quad \text{subject to} \\ d_{R_k} - \mathbf{p}(V) \cdot \mathbf{x} &\leq s, \quad V \subseteq R_k \\ \mathbf{p}(V) \cdot \mathbf{x} - d_T &\geq s, \quad V \subseteq T. \end{aligned} \tag{13}$$

Considering the mapping $\mathbf{F}$ as a composite of the dose mapping $\mathbf{d}$ from the solution space $\mathbb{X}$ containing the intensity vectors $\mathbf{x}$ into the structure space $\mathbb{D}$ of dose vectors $\mathbf{d}$ and the evaluation functions

$$\begin{aligned} f_k : \mathbb{D} &\rightarrow \mathbb{R} \\ \mathbf{d} &\mapsto \max_{V \subseteq R_k} d(V) - d_{R_k} \end{aligned}$$

and

$$\begin{aligned} f_T : \mathbb{D} &\rightarrow \mathbb{R} \\ \mathbf{d} &\mapsto d_T - \min_{V \subseteq T} d(V), \end{aligned}$$

problem (13) can be reformulated in the general environment of design problems as

$$\begin{aligned} s &\rightarrow \min \quad \text{subject to} \\ f_{R_k}(\mathbf{P} \cdot \mathbf{x}) &\leq s \\ f_T(\mathbf{P} \cdot \mathbf{x}) &\geq s. \end{aligned} \tag{14}$$

In this context, the problem asymmetry can be interpreted in the sense, that "the partial derivatives $\frac{\partial}{\partial d(V)} f_k(\mathbf{P}\mathbf{x}^*)$ and $\frac{\partial}{\partial d(V)} f_T(\mathbf{P}\mathbf{x}^*)$" of the evaluation functions in $\mathbf{P}\mathbf{x}^*$ are nonzero only for the voxels V corresponding to relations that are fulfilled with equality.
This concept can be generalized to nonlinear programs in the following way. Consider problem (14) as a nonlinear program with the solution $\mathbf{x}^*$ and assume, that it is asymmetric in the sense that

$$\left| \frac{\partial}{\partial d(V_j)} f_k(\mathbf{P}\mathbf{x}^*) \right| < \varepsilon \tag{15}$$

for most of the voxels V_j, i.e. the vast majority of the partial derivatives of the indicator functions stay below some small error bound $\varepsilon > 0$. Let $\mathbf{P}' = (\mathbf{p}'(V_j))_j \in \mathbb{R}^{\dim(\mathbb{D})\times\dim(\mathbb{X})}$ be an approximation of $\mathbf{P}$. The problem

$$\begin{aligned} s &\rightarrow \min \quad \text{subject to} \\ f_{R_k}(\mathbf{P}'\mathbf{x}) &\leq s \\ f_T(\mathbf{P}'\mathbf{x}) &\geq s \end{aligned} \tag{16}$$

can then be interpreted as an approximation of the original problem (14). According to [12], the optimal value and the solutions of the approximate problem converge to the optimal value and the solutions of the original problem for $\max_j \|\mathbf{p}(V_j) - \mathbf{p}'(V_j)\| \rightarrow 0$. However, for V_j with (15), even larger $\|\mathbf{p}(V_j) - \mathbf{p}'(V_j)\|$ could be easily accepted, since the resulting approximation errors $|\mathbf{p}(V_j) \cdot \mathbf{x}^* - \mathbf{p}'(V_j) \cdot \mathbf{x}^*| \leq \|\mathbf{p}(V_j) - \mathbf{p}'(V_j)\|\|\mathbf{x}^*\|$ do not really affect the value of the indicator functions due to (15).
This provides the following conclusion: if one had an approximation $\mathbf{P}'$ of $\mathbf{P}$, for which $\mathbf{P}' \cdot \mathbf{x}$ could be cheaply computed with acceptable errors in the entries for which (15) holds, and exact values only in the very few others, then the optima of the corresponding approximate problem (16) would be also (almost) optimal for the original problem (14), but could be obtained with a much smaller computational expense.
Concerning IMRT, the inverse treatment planning problems are asymmetric in the above terminology. However, in contrast to ordinary discrete optimization problems, the continuous background of this problem provides a possibility to exploit the asymmetry by constructive means: voxels lying in the vicinity of each other are irradiated similarly by most of the beamlets and thus play a similar role in the optimization. This means, for a fixed dose distribution $\mathbf{d}$, critical voxels with a strong influence on the quality of the dose distribution respectively the evaluation function will concentrate in local volume parts. Analogously, the error bound (15) will also typically be fulfilled by such neighboring voxels. Furthermore, the shape of these critical parts of the body volume varies more or less continuously in $\mathbf{d}$. Hence, knowledge on all these aspects allows a highly efficient construction of an approximate $\mathbf{P}'$, as done using the adaptive clustering method.

5 Navigating the data base

When the plan database computation is finished, a vital part of the planning is not yet accomplished. The planner still has to select a favourite solution. Since inspecting a plan usually involves sifting through all its slices a manual inspection of all plans contained in the database is infeasible.
The idea is to use an interactive multicriteria optimization method that works on blends of the pre-computed plans only. User actions are trans-

formed into optimization problems on this restricted domain. The restriction of domain together with the structural information gained during the calculation of the database allows the problems to be solved in real-time. Therefore, the execution of the interactive method feels more like navigation than optimization. Note that the strategy we propose does not possess any of the shortcomings of a Human Iteration Loop we mentioned in section 2 (see 5.5 for a more detailed discussion).
The feeling of direct control is strengthened by constantly providing the user with a visualization of the current solution and up to date estimates of the ideal point - the combination of the individual minima - and the Nadir point - the combination of the individual maxima of the indicator functions over the current domain. Having thus a clear picture of the possibilities and limitations the planner's forthcoming decisions are based on a much firmer ground.

There are two basic mechanisms in our interactive method (patented for radiotherapy planning by the Fraunhofer ITWM [40]):

- the *restriction* mechanism that changes the feasible region and
- a Tchebycheff problem based search mechanism called *selection*.

The former updates the ideal and Nadir point estimates after a change to the box constraints for the indicator functions and is used to exclude unwanted parts of the domain-restricted problem's Pareto boundary. The latter searches for a plan that best adheres to a planner's wish.
A special variant of the restriction mechanism is the use of a *lock*, which is a shortcut for restricting the chosen indicator function to the current or better values. Furthermore, the whole database can be re-normalized, i.e. all plans can be scaled to a new mean dose in the target.
Miettinen [26] lists several other methods for interactive approaches, including some remarks on useful visual displays. However, none of these taken alone serve the purpose we set out to fulfill.

5.1 The restriction mechanism

The restriction mechanism allows the planner to set feasible hard constraints on the indicator function values a posteriori. Let $\hat{\mathcal{X}} := conv\left\{\mathbf{x}^{(l)}, l \in \mathcal{L}\right\}$ be the feasible region and $\mathcal{X}_{\mathbf{u}} := \left\{\mathbf{x} \in \hat{\mathcal{X}} : \mathbf{F}(\mathbf{x}) \leq \mathbf{u}\right\}$ be the set of solutions that are feasible for the current box constraints.
Every change in the right hand side of the box constraints $\mathbf{F}(\mathbf{x}) \leq \mathbf{u}$ causes the system to update its estimate of the ideal and Nadir point, thus providing the planner with a the so called *planning horizon* - the multidimensional interval between the ideal and Nadir point estimate.

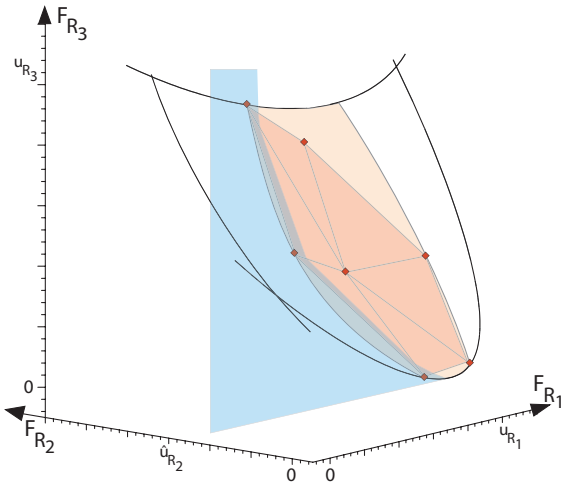

Figure 19: A new upper bound for F_{R_2} is introduced.

5.1.1 Minimum values - the ideal point

Let us now introduce some notation. The calculated plans' fluence maps $\mathbf{x}^{(l)}, l \in \mathcal{L}$ are combined into a matrix $\mathbf{X} := \left(\mathbf{x}^{(l)}\right)_{l\in\mathcal{L}}$ with columns consisting of the fluence maps. Likewise, the indicator function vectors $\mathbf{y}^{(l)} := \mathbf{F}(\mathbf{x}^{(l)}), l \in \mathcal{L}$ are combined into a matrix $\mathbf{Y} = \left(\mathbf{y}^{(l)}\right)_{l\in\mathcal{L}}$. Thus, the entry (l, k) of $\mathbf{Y}$ represents the k^{th} indicator function value of the l^{th} solution.
As the change of an upper bound in some indicator function changes the feasible region, it may alter the minima of the indicator functions as well. If the upper bound $\mathbf{u}$ changes the new ideal point can be found by solving the following problem for each indicator function $F_k \in \mathcal{K}$:

$$\begin{aligned} F_k(\mathbf{X}\boldsymbol{\lambda}) &\rightarrow \min \quad \text{subject to} && (17)\\ \mathbf{F}(\mathbf{X}\boldsymbol{\lambda}) &\leq \mathbf{u} && (18)\\ \boldsymbol{\lambda} &\in \Sigma, \end{aligned}$$

where $\Sigma := \left\{\boldsymbol{\lambda} \in \mathbb{R}_+^{|\mathcal{L}|} : \mathbf{e}^T\boldsymbol{\lambda} = 1\right\}$ is the simplex of convex combination coefficients.
The optimization problem (17) finds a convex combination of the stored solutions, minimizing the k^{th} indicator function, while observing the bounds $\mathbf{u}$.
Problem (17) is convex because the functions F_k are convex and can therefore be efficiently solved. However, it is not clear a priori how fast these problems can be solved - at least it is not known if they can be solved fast enough to allow a real-time navigation. Hence, a linear approximation of (17) is formulated as:

$$
\begin{aligned}
(\mathbf{Y}\boldsymbol{\lambda})_k &\rightarrow \min \quad \text{subject to} && (19)\\
\mathbf{Y}\boldsymbol{\lambda} &\leq \mathbf{u}\\
\boldsymbol{\lambda} &\in \Sigma. && (20)
\end{aligned}
$$

The linear problem (19) overestimates the true minimum since

$$\mathbf{Y}\boldsymbol{\lambda} = \left(\mathbf{F}(\mathbf{x}^{(l)})\right)_{l\in\mathcal{L}}\boldsymbol{\lambda} \geq \mathbf{F}(\mathbf{X}\boldsymbol{\lambda}) \tag{21}$$

due to convexity. Therefore, the feasible set of problem (19) $\Lambda' := \{\boldsymbol{\lambda} \in \Sigma \mid \mathbf{Y}\boldsymbol{\lambda} \leq \mathbf{u}\}$ is contained in the feasible set of the original problem (17):

$$\Lambda' \subseteq \Lambda := \{\boldsymbol{\lambda} \in \Sigma \mid F(\mathbf{X}\boldsymbol{\lambda}) \leq \mathbf{u}\} \tag{22}$$

So the LP works on a subset of the original domain and in addition to that its objective function is due to convexity larger than the original convex objective function. Therefore, the result gives an upper bound for the true minimum.
Depending on the computational complexity of the original formulation, one can either solve the original problems for the individual minima or use the linear estimates.

5.1.2 Maximum values - the Nadir point

A different problem is faced in finding the maximum values of the indicator functions. For this, let $\hat{\mathbf{u}}$ be the vector of the individual maxima contained in the database, i.e. $\hat{u}_i := \max_{l\in\mathcal{L}} \left\{y_i^{(l)}\right\}$. It can easily be shown that this is the Nadir point of the multicriteria problem restricted to $\hat{\mathcal{X}}$. From the definitions it directly follows that $\hat{\mathcal{X}} = \mathcal{X}_{\hat{\mathbf{u}}}$.
However, for general u the situation is not as straight forward. The problem formulation to obtain the k^{th} coordinate of the new Nadir point reads:

$$
\begin{aligned}
F_k(\mathbf{X}\boldsymbol{\lambda}) &\rightarrow \max \quad \text{subject to} && (23)\\
\mathbf{F}(\mathbf{X}\boldsymbol{\lambda}) &\leq \mathbf{u}\\
\boldsymbol{\lambda} &\in \Sigma
\end{aligned}
$$

Using the same linearization strategy for the ideal point yields

$$
\begin{aligned}
(\mathbf{Y}\boldsymbol{\lambda})_k &\rightarrow \max \quad \text{subject to} && (24)\\
\mathbf{Y}\boldsymbol{\lambda} &\leq \mathbf{u}\\
\boldsymbol{\lambda} &\in \Sigma
\end{aligned}
$$

as an estimate for the k^{th} Nadir point coordinate.
The feasible region Λ' in (24) is a subset of the feasible region Λ in (23) potentially reducing the maximum, but the objective function $(\mathbf{Y}\boldsymbol{\lambda})_k$ overestimates the true function value. Therefore, the two approximations have contradicting effects which might produce inconsistent results. Evaluating $F_k(\mathbf{X}\boldsymbol{\lambda}^{(k)})$ for the optimum $\boldsymbol{\lambda}^{(k)}$ of the LP, however, corrects the second effect and yields the conservative estimate we are looking for.

Unlike the problem of finding the ideal point the Nadir point problem cannot easily be solved in its original formulation, since it is a convex maximization problem. Hence, there are multiple local optima.
In literature there are different methods of estimating the Nadir point. Our method uses a lot of problem structure and shows good practical behaviour combined with low computational complexity, making it a good choice for our purposes.

5.2 The selection mechanism

So far, the user can only manipulate the planning horizon but cannot change the currently chosen solution. This is done with the second mechanism, the selection. The first solution presented to the user could be any plan from the database. Usually, the equibalanced solution is shown, i.e. the solution to problem 11 (see page 21).
The user can now change one of the indicator function values of the current solution within the bounds given by the ideal and Nadir point estimates and the system searches for a solution that attains the chosen value in the chosen indicator function and changes the other indicator function values least possible.
This search is accomplished by solving a Tchebycheff problem for a specifically chosen reference point:
Since the starting point for the selection mechanism $\hat{\mathbf{y}}$ is assumed to be Pareto optimal in $\mathcal{Y}_u$, there exists a weighting vector $\hat{\mathbf{n}} \in int\left(\mathbb{R}_+^{|\mathcal{K}|}\right)$, $\|\hat{\mathbf{n}}\|_2 = 1$ with

$$\hat{\mathbf{n}}^T\,\hat{\mathbf{y}} \leq \hat{\mathbf{n}}^T\,\mathbf{y} \quad \forall \mathbf{y} \in \mathcal{Y}_u$$

This vector is a subgradient of the Pareto boundary at $\hat{\mathbf{y}}$ and can be found by calculating a subgradient of the scalarization function at $\hat{\mathbf{y}}$.
Now, let k be the index of the changed indicator and $\mathbf{e}_k$ be the k^{th} unit vector. Let

$$\begin{aligned} \bar{\mathbf{r}} &:= \mathbf{e}_k - \mathbf{e}_k^T\hat{\mathbf{n}}\,\hat{\mathbf{n}} \\ &= \mathbf{e}_k - \hat{\mathbf{n}}_k\hat{\mathbf{n}} \\ &> 0 \quad \text{, since } \hat{\mathbf{n}} \in int\left(\mathbb{R}_+^{|\mathcal{K}|}\right) \end{aligned}$$

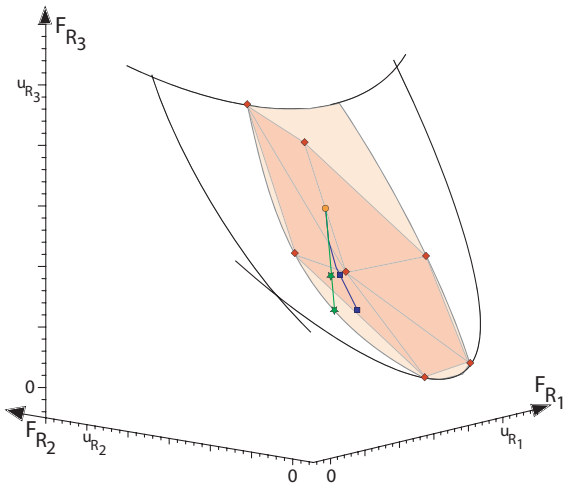

Figure 20: The straight line where the reference points are chosen from (asterisks) and the corresponding solutions (squares) found in the optimization problem (26).

Now $\mathbf{r} := \frac{\bar{\mathbf{r}}}{\bar{r}_k}$. Then $\hat{\mathbf{y}}$ and $\mathbf{r}$ describe the line on which the reference point $\bar{\mathbf{y}}$ is chosen. As this line is contained in a supporting hyperplane, $\bar{\mathbf{y}}$ is not dominated by any point in $\mathcal{Y}_{\mathbf{u}}$. Therefore, absolute values are unnecessary in the formulation of the Tchebycheff problem.
Let μ be the value chosen for $\mathbf{F}_k$, then the selection mechanism problem is formulated as

$$\begin{aligned} \|\mathbf{F}(\mathbf{X}\boldsymbol{\lambda}) - \bar{\mathbf{y}}(\mu)\|_\infty &\rightarrow \min \quad \text{subject to} \\ \mathbf{F}(\mathbf{X}\boldsymbol{\lambda}) &\leq \mathbf{u} \\ F_k(\mathbf{X}\boldsymbol{\lambda}) &= \mu \\ \boldsymbol{\lambda} &\in \Sigma \end{aligned} \tag{25}$$

where $\bar{\mathbf{y}}(\mu) := \hat{\mathbf{y}} + (\mu - \hat{y}_k)\mathbf{r}$. Approximating again $\mathbf{F}(\mathbf{X}\boldsymbol{\lambda})$ by $\mathbf{Y}\boldsymbol{\lambda}$, we attain the linear approximation

$$\begin{aligned} \|\mathbf{Y}\boldsymbol{\lambda} - \bar{\mathbf{y}}(\mu)\|_\infty &\rightarrow \min \quad \text{subject to} \\ \mathbf{Y}\boldsymbol{\lambda} &\leq \mathbf{u} \\ (\mathbf{Y}\boldsymbol{\lambda})_k &= \mu \\ \boldsymbol{\lambda} &\in \Sigma \end{aligned} \tag{26}$$

The resulting linear program (26) is solved using a Simplex algorithm. Since the LP has $|\mathcal{K}| + 1$ constraints, any basic feasible solution in the Simplex'

iterations has at most $|\mathcal{K}| + 1$ non-zero elements. Therefore, only $|\mathcal{K}| + 1$ plans enter the convex combination, making the complexity of executing the convex combination predictable and in particular independent of the number of plans in the database.
Due to convexity $\mathbf{F}(\mathbf{X}\boldsymbol{\lambda}) \leq \mathbf{Y}\boldsymbol{\lambda}$ so that possibly $(\mathbf{Y}\boldsymbol{\lambda})_k < \mu$ (see also figure 14, page 25). If the deviation from the equality constraint is too large, one can use a column generation process to improve the approximation:
The matrix $\mathbf{Y}$ is augmented by $\mathbf{F}(\mathbf{X}\boldsymbol{\lambda})$ and the dimension of the vector $\boldsymbol{\lambda}$ is enlarged by one. This results in an improved approximation of the boundary of $\mathcal{Y}_\mathbf{u}$, thus improving the accuracy of the equality constraint.
The problem (26) implicitely describes a path on the Pareto boundary parameterized by μ (cf. fig 20). Since the direction $\mathbf{r}$ depends on the starting point a backward move started from the end point of one selection mechanism result does in general not yield the original starting point. This is due to the problem formulation that tries to distribute load and benefit equally among the indicator function values based on a local prediction. As the local prediction changes with the starting point, so does the way of distributing load and benefit.

Depending on the time restrictions and the problem complexity, the solution found through navigation could be used as a starting point for a post-optimization to move it to the Pareto boundary of the original problem. To accomplish this, a combination of the ε-constraint method and weighted sum or weighted metric method could be used. The point gained can then be added to the database improving the local approximation of $\mathcal{Y}_\mathbf{u}$'s Pareto boundary.

5.3 Possible extensions to the navigation

It should be mentioned here that the navigation is versatile. There is a lot of possible additional functionality. It is, for example, possible to add or delete indicator functions at any point during the planning process. Of course having added a new indicator function, the solutions in the database are not Pareto optimal with respect to the new set of functions over the original domain $\mathcal{X}$, but they can at least be evaluated under the additional criterion.
The new indicator function may then of course be considered in the navigation and the navigation still selects the best possible choices over the restricted domain $\hat{\mathcal{X}}$. Using post-optimization the approximation of the now higher dimensional Pareto boundary can again be locally improved, yielding a good local picture of the new Pareto boundary, but revealing an incomplete global picture, i.e. potentially bad estimates for the ideal and Nadir point.

The navigation is independent of the way the plans in the database were

created. Hence, the database could stem from several manually set up optimizations and the navigation then allows to mix them. This is in particular relevant, if the clinical case is well known and the computation of a whole bundle of plans, i.e. the extreme compromises plus additional plans seems needless.
The independence from the creation process enables the addition of plans at any stage. Therefore, single solutions could be added even after the computation of a bundle. So bundle computations can be combined with manually set up plans in arbitrary sequence.

5.4 The user interface for the navigation

The described workflow is a destinct improvement compared to something like an human iteration loop (cf. chapter 2). For implementing the improved workflow, an appropriate visualization and manipulation tool is needed. Its interface has to support the navigation of the database's *continuous* Pareto boundary in real-time, and be able to visualize the results concurrently.
Using all plans from $\mathcal{X}_u$ the number of alternative solutions is not artificially limited due to any form of discretization. Ideally, the only form of discretization should stem from precision of the pointing devices or the display.

The navigation screen (see figure 21) is divided into two parts. The left hand side visualizes the database as a whole and embeds the current solution into the database. The right hand side displays the current plan's dose volume histogram and the dose distribution on transversal, frontal and sagittal slices.
The star on the left hand side is composed of axes for all currently selected critical structures. The interval on the axes corresponds to the indicator function value's range contained in the database for the respective structure. The white polygon marks the indicator function values for the currently selected plan.
The shaded area represents the *planning horizon*. It is subdivided into the *active* and the *inactive* planning horizon. The latter is the range between minimum and maximum value contained in the database and the former is bounded on each axis by the maximum and minimum values implied by the currently set restrictions. Note that the line connecting the minimum values of the active planning horizon is the current ideal point estimate and the line connecting the maximum values is the current estimate for the Nadir point.
The line representing the currently selected plan has a handle bar called *selector* at each intersection with an axis. The right hand side of the screen displays the plans that are found while the selector is moved. The axes also contain *restrictors* by which the upper bounds for the active planning horizon can be changed.

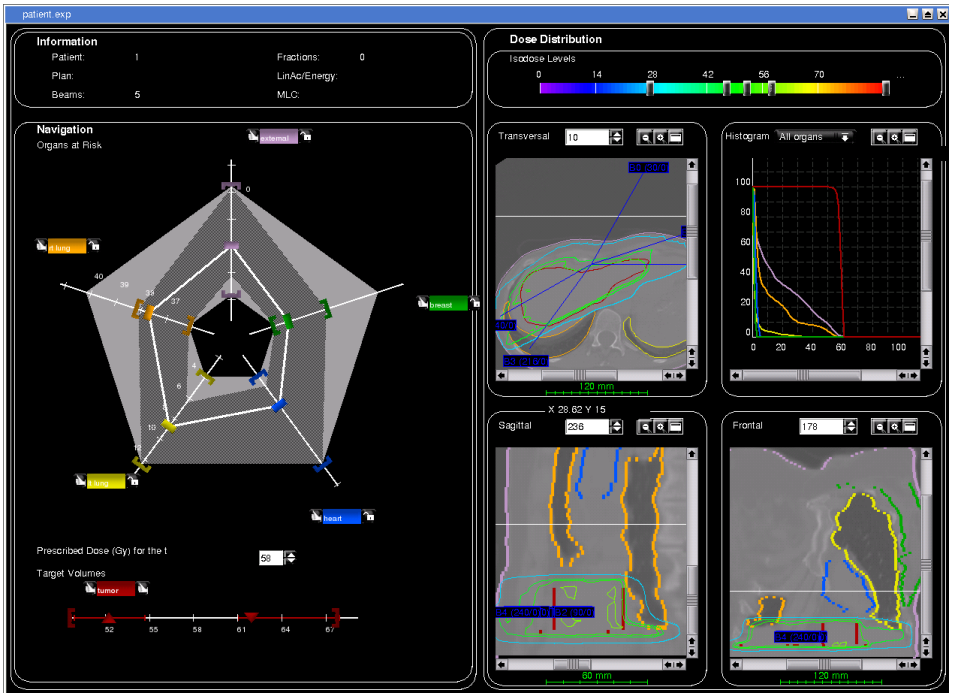

Figure 21: The navigation screen. The star on the left hand side with the active and inactive planning horizon and the current solution. On the right the dose visualization and the dose volume histogram.

The visualization is updated several - usually around seven - times a second when a selector or restrictor is moved, so the user gets immediate feedback about the consequences of his or her decisions. This means that around 7 linear problems of type (26) respectively $7 * |\mathcal{K}|$ linear problems of type (19) and (24) are solved every second when the user pulls a selector or restrictor. So, instead of waiting for the consequences of a parameter adjustment the planner immediately sees the outcome.

5.5 Concluding remarks on decision-making

One of the critiques against the conventional techniques in treatment planning is that the models are fixed at design time. As it is possible to extend our navigation scheme by new indicator functions, our approach does not suffer from being inflexible in modeling the problem.

We demonstrated in section 2 that a decision-making process that is capable of conveying the shape of the Pareto boundary leads to more stability in how the solutions are conceived by the decision-maker.
The method we propose aids the decision-maker to explore different prefer-

ence structures while reaching a decision. The method we propose demonstrates the possibilities and limitations of the solutions in terms of the ideal and Nadir point in real-time. In this sense, the user gets a feel for the interdependencies of the different indicator functions.
Watching the reaction of the other indicator functions during a selection operation on the other hand gives a planner a feeling for the local trade-off, i.e. the steepness of the Pareto-boundary around the starting point.
Furthermore, the trade-offs involved can be explicitly calculated in terms of the gradient information which is readily available from the optimization problems that constitute the database and can consequently be visualized as a lookahead for the forthcomming changes.
By communicating the above information to the decision-maker, the tool conveys more information about the feasible outcomes of the problem, and thus a much more informed decision can be made, of course.

In summary, the decision-making process for the treatment planning problem described in this paper handles the multicriterial aspects of the problem more directly than conventional approaches.

6 Clinical examples

This chapter presents the new multicriterial optimization paradigm as it can be realized in daily clinical practice. We will illustrate the new multicriterial treatment planning by two clinical cases representing the most important indications for IMRT, namely prostate and head and neck cancer.

6.1 Prostate cancer

Prostate cancer is the most frequent cancer in men in the western world. Studies showed that prostate cancer patients with still localized disease but a high risk (which is derived from a histological grading score and the concentration of the prostate specific antigen, PSA) will benefit from a high dose prostate irradiation. However, this dose is limited by the rectum which is located directly dorsal to the prostate, implying the risk of rectal bleeding and incontinence [30].

Using IMRT instead of conventional radiotherapy, the dose distribution can be better tailored to the target volume, lowering the rectum toxicity [50]. But even with IMRT, every treatment plan will be a clinical compromise between the dose in the target volume and the dose to the rectum. Other structures involved in prostate treatment planning are the bladder and the femoral heads.

For the sake of simplicity, in the following we will only consider one target volume and the rectum as main contradictory goals for this kind of planning problem. Let us now assume that the planner has defined the organ

contours and the beam geometry. Then the multicriteria planning program calculates the plan database. Since there are only two trade organs, the database consists of the equibalanced solution, two extreme compromises and 17 intermediate plans summing up to 20 solutions, which were computed in 10 minutes. After that the navigator user interface is displayed like it is shown in figure 22.

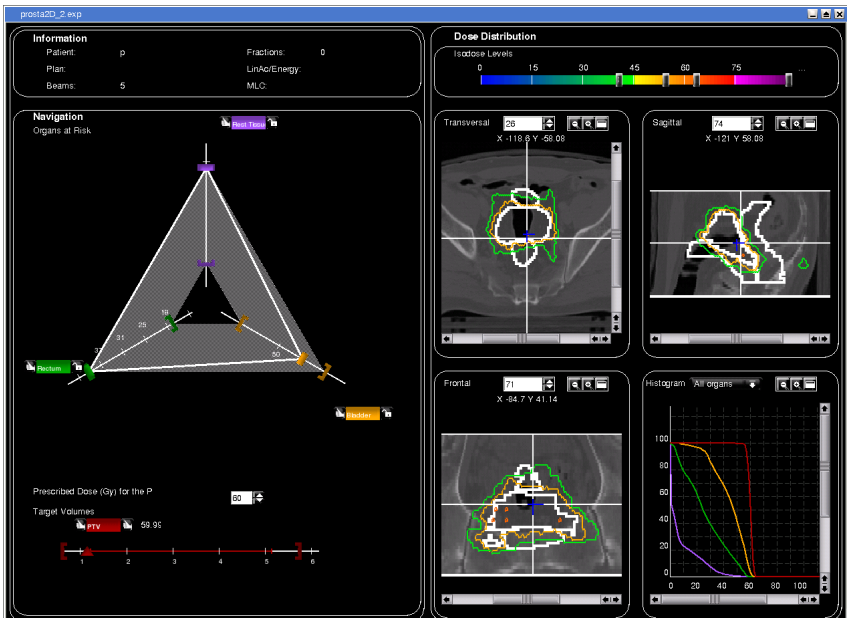

Figure 22: Navigation screen for the prostate example

All plans are normalized to the same mean target dose which greatly facilitates the comparison of different plans, because now only the homogeneity of the target dose distribution, represented by the standard deviation sigma, has to be judged against the rectum dose which is represented by the equivalent uniform dose, EUD.
At first sight, the planning horizon can be seen in the navigation window in Fig 22. In this example the EUD of the rectum reaches from 18.0 Gy to 40.6 Gy. If the lowest dose to one organ at risk is still too high to be acceptable, then the planner knows immediately without any further calculation that the target dose has to be reduced by re-normalizing the database.

Now the interactive planning process begins. By dragging either the target homogeneity slider or the rectum EUD slider with the mouse, the treatment planner can quickly explore all compromises between target dose and rectum dose that are achievable with the given setup geometry.
Because in this case the Pareto front is only two-dimensional, it can also be plotted and shown completely in a graph, see Figure 23.

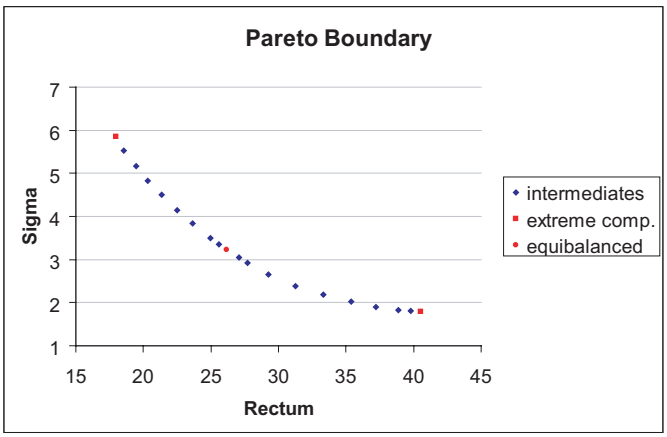

Figure 23: Standard deviation in the target against EUD in the rectum

While dragging one of the navigation sliders, the user wanders along the Pareto frontier, and all information in the navigator window like the isodose distribution and the dose volume histogram is updated in real-time.

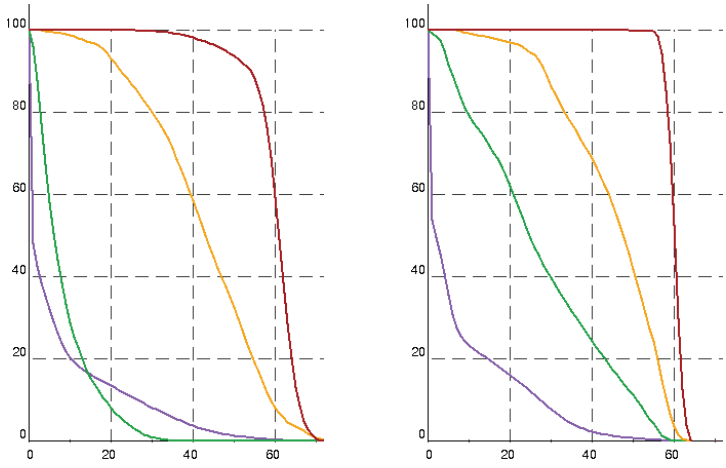

Figure 24: DVH graphs for the extreme compromises

Unfortunately, the dynamics of changing the plan and the effect of direct feedback is impossible to demonstrate in this written paper. Instead, we just plotted the DVHs of the extreme ends of the Pareto boundary, see figure 24 (page 42. In reality there is a smooth transition between these extremes and the planner can decide quickly for the best clinical compromise.

6.2 Head and neck cancer

Treatment planning for head and neck cancer can be a very challenging task. The primary tumor can be located anywhere in the naso- and oropharyngeal area, and regularly the lymphatic nodal stations have to be irradiated because they are at risk of containing microscopic tumor spread. This results in big, irregular shaped target volumes with several organs at risk nearby. The salivary glands are such organs at risk that are quite radio-sensitive. The tolerance dose of the biggest salivary gland, the parotid gland, is approximately a mean dose of 26 Gy [28]. The goal should be to spare at least one of the parotid glands. Otherwise the patient will suffer from xerostomia (a complete dry mouth) which can significantly reduce the quality of life. Other structures that have to be considered are (depending on the specific case) e.g. the brain stem, the spinal cord, the esophagus and the lungs.
If there is macroscopic tumor left, it can be considered as an additional target volume and treated with a higher dose. This is known as simultaneously integrated boost concept (SIB [21], [27]), and further increases the complexity of the planning problem.
In Fig 25(a) the case of a lymphoepithelioma originating from the left Eustachian tube is shown. The database for this case contains 25 solutions and took 11 minutes to be computed. Again, the complete planning horizon can be seen at first sight, and a first solution is presented to the planner.

Now the interactive planning process is basically the same as described for the prostate case. However, because this planning problem is more complex, exploring the Pareto boundary is not as straightforward as in two-dimensional cases. Therefore the program provides the possibility of *locking* or *restricting* an organ to exclude unwanted parts from the navigation. By clicking the *lock* option for a specific structure, all solutions with worse indicator values for the chosen organ than the current one are excluded from the further exploration. This is visualized by a reduced planning horizon, see figure 25(b). It allows for narrowing down the solution space to the area that is of highest clinical relevance. Of course, the lock can be reversed at any time, bringing back the broader planning horizon.
Complex planning problems can be interactively explored this way, and the best clinical solution can be found in a short amount of time.

6.3 General remarks

It is important to note that in daily practice the mathematical details of the implementation as they were described in the previous chapters are almost completely hidden from the treatment planner. Instead, the planner can focus on the clinical aspects of the specific case. This is a crucial requirement for a broad acceptance in the radiooncological community.

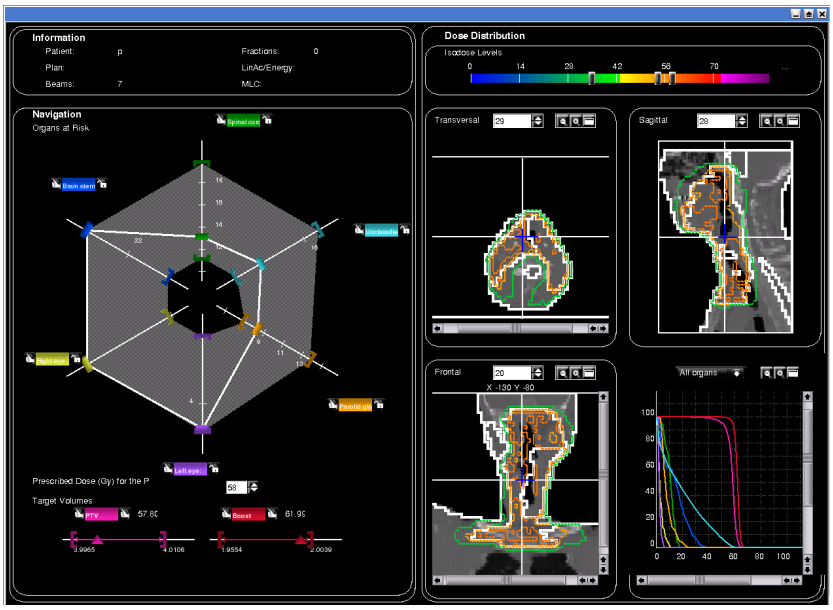

(a) Navigation screen at the beginning of the planning process

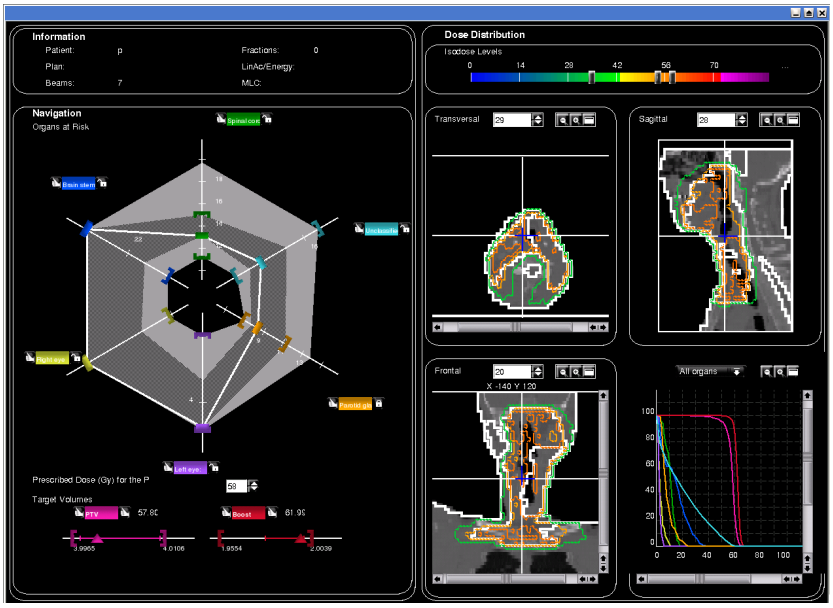

(b) Navigation screen after some restrictions have been made - note the significant difference in the remaining planning domain

Figure 25: Navigation screens for the head and neck case

Since many hospitals worldwide already have introduced IMRT into their clinical routine, the new planning scheme as proposed in this paper also has to be integrated into existing workflows.
Treatment planning in radiotherapy departments is usually a close collaboration between physicians and physicists. After the images for treatment planning were aquired, the outlines of the tumor target volume and the organs at risk are defined. Then the beam geometry and the fluence maps are determined, which is the core part of the treatment planning process. When a certain plan is chosen for treatment, it is dosimetrically verified using hospital-dependent verification procedures, and finally the patient is treated.
Today several commercial IMRT treatment planning programs exist for determining the beam setup and the fluence maps, but all of them share the drawbacks of single-objective optimization mentioned previously. The new multicriteria planning program is able to replace this core part of the workflow while leaving all other parts before and after it unchanged.
The result is an improved plan quality and consequently probably better clinical outcome. At the same time radiotherapy planning is made easier to handle with reduced time requirements, facilitating an even broader introduction of the highly developed IMRT technique in radiotherapy departments.

7 Research topics

While the fluence map optimization is itself a challenging problem, there are still difficulties concerning the application of a planned treatment. Since the optimized fluence maps are to be delivered with the help of a MLC, a sequencing algorithm has to determine the configuration of such hardware - static or dynamic.
Algorithms have been proposed for both types, and there is a lot of literature on this topic. For an excellent survey of existing algorithms, see the paper of Kalinowski [15]. However, only few of the existing approaches explicitly consider technical difficulties like leakage or scattering. There is also the issue of unnecessary long treatment times due to a large number of shapes in the static step-and-shoot method. While there are some theoretical limits as to what can be done (minimization of the number of segments is NP-hard, for example), there is yet some efficiencies and improvements in the accuracy of delivery to be gained.
A much-cited approach to this end has been the incorporation of sequencing into the fluence map optimization problem. Romeijn et al propose a clever Column Generation scheme for the convex planning problem with linear constraints in [34]. Their formulation results in a pricing problem that is structurally very similar to a network formulation proposed in [3].

While it is theoretically possible to maintain a database of already sequenced solutions, it is not meaningful to do so when plans are afterwards blended in a real-time process. If a convex combination of several plans is taken, the sequenced solution can be obtained by a convex combination of the delivery coefficients - the monitor units - in the step-and-shoot method. This will very likely, however, result in a high number of shapes and possible inaccuracies due to technical phenomena like tounge-and-groove effects or unnecessary high leakage errors.
Given a fast sequencing algorithm that is flexible enough to incorporate these physical effects, it may be possible to sequence at least a current representative solution in real-time or nearly real-time.

Another direction is the recent movement towards the dynamic plan adaption to the organ geometry known as adaptive or 4D planning [47, 18]. During a treatment the organ geometry in a patient changes. The impact of an altered geometry to the quality of a plan may be detrimental if target regions meant to receive high dose are close to critical structures. These changes are usually grouped into the *inter fraction* [25, 36, 47, 45, 46] and *intra fraction* [18, 19, 23, 24, 31, 41, 52] changes.

The former are due to the patient losing weight or the tumor becoming smaller over the time of treatment. They may be reacted upon by a short re-optimization of the existing plans. The old plans should provide excellent starting points in the optimization given that the changes are on a relatively small scale.

The latter are due to breathing or digestion and are harder to tackle. Some approaches try to anticipate forthcoming changes and incorporate that into the planning. Doing so the optimization is very similar to the planning for inter fraction changes.
The complications faced by any reactive scheme that monitors the movements of all critical structure during treatment and adjusts the plans online are more involved. One possible distinction between these movements might be into periodic movements (e.g. breathing) and random or unforeseen movements.
If the movements can be categorized into periods and certain "typical" states can be established for each period, then the plan adaptation could be parametrized by these periods. If, for example, the critical structures in the chest are known to be in a similar arrangement for each of the breathing periods defined, the patient could be monitored for the current period and the treatment follows the corresponding plan until the next period is reached. Of course, care has to be taken to find plan parametrizations that are feasible within the short time frames between periods. Also, a sufficiently fine monitoring device must be installed for such an adaptation.
While the unforeseen movements could in principle be treated analogously, true online optimization is necessary as a parametrization would not exist.

Here again, the question is for feasible methods that operate in very short time frames. In the future, however, with increasing sophistication of the devices used to deliver treatment, these questions need consideration and practical answers.

Literatur

[1] MS Bazaraa, HD Sherali, and CM Shetty. *Nonlinear Programming - Theory and Algorithms*. John Wiley and Sons, 1993.

[2] HP Benson and E Sun. Pivoting in an outcome polyhedron. *Journal of Global Optimization*, 16:301–323, 2000.

[3] N Boland, HW Hamacher, and F Lenzen. Minimizing beam-on time in cancer radiation treatment using multileaf collimators. *Networks*, 43(4):226–240, 2004.

[4] TR Bortfeld. Dosiskonformation in der Tumortherapie mit externer ionisierender Strahlung: Physikalische Möglichkeiten und Grenzen. *Habilitationsschrift, Deutsches Krebsforschungszentrum, Heidelberg*, 1995.

[5] TR Bortfeld, J Stein, and K Preiser. Clinically relevant intensity modulation optimization using physical criteria. In D.D. Leavitt and G. Starkschall, editors, *Proceedings of the XIIth ICCR*, Salt Lake City, 1997.

[6] A Brahme. Dosimetric precision requirements in radiation therapy. *Acta Radiol Oncol*, 23:379–391, 1984.

[7] A Brahme. Treatment optimization using physical and radiobiological objective functions. In A Smith, editor, *Radiation Therapy Physics*. Springer, Berlin, 1995.

[8] RE Burkard, H Leitner, R Rudolf, T Siegl, and E Tabbert. Discrete optimization models for treatment planning in radiation therapy. In H Hutten, editor, *Science and Technology for Medicine, Biomedical Engineering in Graz*, Pabst, Lengerich, 1995.

[9] I Das. An improved technique for choosing parameters for pareto surface generation using normal-boundary intersection. In *WCSMO-3 Proceedings, Buffalo, NY*, 1999.

[10] Jerald P. Dauer. Analysis of the Objective Space in Multiple Objective Linear Programming. *J Math Anal Appl*, 126:579–593, 1987.

[11] B Emami, J Lyman, A Brown, L Coia, M Goitein, JE Munzenrieder, B Shank, LJ Solin, and M Wesson. Tolerance of normal tissue to therapeutic irradiation. *Int J Radiat Oncol Biol Phys*, 21:109–122, 1991.

[12] AY Fiacco. *Introduction to Sensitivity and Stability Analysis in Nonlinear Programming*, volume 165 of *Mathematics in Science and Engineering*. Academic Press, 1983.

[13] AM Geoffrion. Proper efficiency and the theory of vector maximization. *J Math Anal Appl*, 22:618–630, 1968.

[14] A Gustafsson, BK Lind, and A Brahme. A generalized pencil beam algorithm for optimization of radiation therapy. *Med Phys*, 21(3):343–356, 1994.

[15] T Kalinowski. Realization of intensity modulated radiation fields using multileaf collimators. *Preprint 03/9, Fachbereich Mathematik, Universität Rostock*, 2003.

[16] I Kaliszewski and W Michalowski. Generation of outcomes with selectively bounded trade-offs. *Foundations of Computing and Decision Sciences*, 20(2):113–122, 1995.

[17] I Kaliszewski and W Michalowski. Efficient solutions and bounds on tradeoffs. *Journal of Optimization Theory and Applications*, 94(2):381–394, 1997.

[18] P Keall. 4-dimensional computed tomography imaging and treatment planning. *Semin Radiat Oncol*, 14:81–90, 2004.

[19] P Keall, V Kini, S Vedam, and R Mohan. Motion adaptive x-ray therapy: a feasibility study. *Phys Med Biol*, 46:1–10, 2001.

[20] KH Küfer, A Scherrer, MP Monz, FV Alonso, H Trinkaus, TR Bortfeld, and C Thieke. Intensity-modulated radiotherapy - a large scale multicriteria programming problem. *OR Spectrum*, 25:223–249, 2003.

[21] A Lauve, M Morris, R Schmidt-Ullrich, Q Wu, R Mohan, O Abayomi, D Buck, D Holdford, K Dawson, L Dinardo, and E Reiter. Simultaneous integrated boost intensity-modulated radiotherapy for locally advanced head-and-neck squamous cell carcinomas: Ii–clinical results. *Int J Radiat Oncol Biol Phys*, 60(2):374–387, 2004.

[22] EK Lee, T Fox, and I Crocker. Beam geometry and intensity map optimization in IMRT via mixed integer programming. *submitted to Int J Radiat Oncol Biol Phys*, 2003.

[23] DA Low, M Nystrom, E Kalinin, P Parikh, JF Dempsey, JD Bradley, S Mutic, SH Wahab, T Islam, G Christensen, DG Politte, and BR Whiting. A method for the reconstruction of four-dimensional synchronized ct scans acquired during free breathing. *Med Phys*, 30:1254–1263, 2003.

[24] AE Lujan, JM Balter, and RK Ten Haken. A method for incorporating organ motion due to breathing into 3d dose calculations in the liver: sensitivity to variations in motion. *Med Phys*, 30:2643–2649, 2003.

[25] AA Martinez, D Yan, D Lockman, D Brabbins, K Kota, M Sharpe, DA Jaffray, F Vicini, and J Wong. Improvement in dose escalation using the process of adaptive radiotherapy combined with three-dimensional conformal or intensity-modulated beams for prostate cancer. *Int J Radiat Oncol Biol Phys*, 50(5):1226–1234, 2001.

[26] K Miettinen. *Nonlinear Multiobjective Optimization*. Kluwer, Boston, 1999.

[27] R Mohan, W Wu, M Manning, and R Schmidt-Ullrich. Radiobiological considerations in the design of fractionation strategies for intensity-modulated radiation therapy of head and neck cancers. *Int J Radiat Oncol Biol Phys*, 46(3):619–630, 2000.

[28] MW Munter, CP Karger, SG Hoffner, H Hof, C Thilmann, V Rudat, S Nill, M Wannenmacher, and Debus J. Evaluation of salivary gland function after treatment of head-and-neck tumors with intensity-modulated radiotherapy by quantitative pertechnetate scintigraphy. *Int J Radiat Oncol Biol Phys*, 58(1):175–184, 2004.

[29] A Niemierko. Reporting and analyzing dose distributions: a concept of equivalent uniform dose. *Med Phys*, 24:103–110, 1997.

[30] A Pollack, GK Zagars, JA Antolak, DA Kuban, and Rosen II. Prostate biopsy status and psa nadir level as early surrogates for treatment failure: analysis of a prostate cancer randomized radiation dose escalation trial. *Int J Radiat Oncol Biol Phys*, 54(3):677–685, 2002.

[31] E Rietzel, GTY Chen, NC Choi, and CG Willett. Four-dimensional image-based treatment planning: target volume segmentation and dose calculation in the presence of respiratory motion. *Int J Radiat Oncol Biol Phys*, 61:1535–1550, 2005.

[32] DF Rogers, RD Plante, RT Wong, and JR Evans. Aggregation and disaggregation techniques and methodology in optimization. *Operations Research*, 39(4):553–582, 1991.

[33] EH Romeijn, RK Ahuja, and JF Dempsey. A new linear programming approach to radiation therapy treatment planning problems. *technical report, Department of Industrial and Systems Engineering, University of Florida, Gainesville, Florida*, 2003.

[34] EH Romeijn, RK Ahuja, JF Dempsey, and A Kumar. A column generation approach to radiation therapy planning using aperture modulation. *technical report, Department of Industrial and Systems Engineering, University of Florida, Gainesville, Florida*, 2003.

[35] EH Romeijn, JF Dempsey, and JG Li. A unifying framework for multicriteria fluence map optimization models. *Phys Med Biol*, 49:1991–2013, 2004.

[36] B Schaly, JA Kempe, GS Bauman, JJ Battista, and J Van Dyk. Tracking the dose distribution in radiation therapy by accounting for variable anatomy. *Phys Med Biol*, 49(5):791–805, 2004.

[37] A Scherrer, KH Küfer, TR Bortfeld, MP Monz, and FV Alonso. IMRT planning on adaptive volume structures - a decisive reduction in computational complexity. *Phys Med Biol*, 50:2033–53, 2005.

[38] W Schlegel and A Mahr. 3D Conformal Radiation Therapy - Multimedia Introduction to Methods and Techniques. Multimedia CD-ROM, Springer, 2001.

[39] R Steuer. *Multicriteria Optimization: Theory, Computation and Applications*. Wiley, NewYork, 1985.

[40] H Trinkaus and KH Küfer. *Vorbereiten der Auswahl von Steuergrößen für eine zeitlich und räumlich einzustellende Dosisverteilung eines Strahlengerätes*. Fraunhofer Institut für Techno- und Wirtschaftsmathematik. Patent erteilt am 8. Mai 2003 unter DE 101 51 987 A.

[41] A Trofimov, E Rietzel, HM Lu, B Martin, S Jiang, GTY Chen, and TR Bortfeld. Temporo-spatial imrt optimization: concepts, implementation and initial results. *Phys Med Biol*, 50:2779–2798, 2005.

[42] AR Warburton. Quasiconcave vector maximation: Connectedness of the sets of pareto-optimal alternatives. *Journal of Optimization Theory and Applications*, 40:537–557, 1983.

[43] S Webb. *The physics of conformal radiotherapy*. IOP Publishing Ltd, 1997.

[44] S Webb. *Intensity-Modulated Radiation Therapy*. IOP Publishing Ltd, 2001.

[45] D Yan, DA Jaffray, and JW Wong. A model to accumulate fractionated dose in a deforming organ. *Int J Radiat Oncol Biol Phys*, 44:665–675, 1999.

[46] D Yan and D Lockman. Organ/patient geometric variation in external beam radiotherapy and its effects. *Med Phys*, 28:593–602, 2001.

[47] D Yan, F Vicini, J Wong, and A Martinez. Adaptive radiation therapy. *Phys Med Biol*, 42:123–132, 1997.

[48] PL Yu. A class of solutions for group decision problems. *Management Science*, 19(8):936–946, 1973.

[49] C Zakarian and JO Deasy. Beamlet dose distribution compression and reconstruction using wavelets for intensity modulated treatment planning. *Med Phys*, 31(2):368–375, 2004.

[50] MJ Zelefsky, Z Fuks, M Hunt, Y Yamada, C Marion, CC Ling, H Amols, ES Venkatraman, and Leibel SA. High-dose intensity modulated radiation therapy for prostate cancer: early toxicity and biochemical outcome in 772 patients. *Int J Radiat Oncol Biol Phys*, 53(5):1111–1116, 2002.

[51] M Zeleny. Compromise programming. In J.L. Cochrane and M. Zeleny, editors, *Multiple Criteria Decision Making*, pages 262–301. University of South Carolina Press, Columbia, South Carolina, 1973.

[52] T Zhang, R Jeraj, H Keller, W Lu, GH Olivera, TR McNutt, TR Mackie, and B Paliwal. Treatment plan optimization incorporating respiratory motion. *Med Phys*, 31:1576–1586, 2004.

Published reports of the Fraunhofer ITWM

The PDF-files of the following reports are available under:
www.itwm.fraunhofer.de/de/zentral__berichte/berichte

1. D. Hietel, K. Steiner, J. Struckmeier

A Finite - Volume Particle Method for Compressible Flows

We derive a new class of particle methods for conservation laws, which are based on numerical flux functions to model the interactions between moving particles. The derivation is similar to that of classical Finite-Volume methods; except that the fixed grid structure in the Finite-Volume method is substituted by so-called mass packets of particles. We give some numerical results on a shock wave solution for Burgers equation as well as the well-known one-dimensional shock tube problem.
(19 pages, 1998)

2. M. Feldmann, S. Seibold

Damage Diagnosis of Rotors: Application of Hilbert Transform and Multi-Hypothesis Testing

In this paper, a combined approach to damage diagnosis of rotors is proposed. The intention is to employ signal-based as well as model-based procedures for an improved detection of size and location of the damage. In a first step, Hilbert transform signal processing techniques allow for a computation of the signal envelope and the instantaneous frequency, so that various types of non-linearities due to a damage may be identified and classified based on measured response data. In a second step, a multi-hypothesis bank of Kalman Filters is employed for the detection of the size and location of the damage based on the information of the type of damage provided by the results of the Hilbert transform.
Keywords: Hilbert transform, damage diagnosis, Kalman filtering, non-linear dynamics
(23 pages, 1998)

3. Y. Ben-Haim, S. Seibold

Robust Reliability of Diagnostic Multi-Hypothesis Algorithms: Application to Rotating Machinery

Damage diagnosis based on a bank of Kalman filters, each one conditioned on a specific hypothesized system condition, is a well recognized and powerful diagnostic tool. This multi-hypothesis approach can be applied to a wide range of damage conditions. In this paper, we will focus on the diagnosis of cracks in rotating machinery. The question we address is: how to optimize the multi-hypothesis algorithm with respect to the uncertainty of the spatial form and location of cracks and their resulting dynamic effects. First, we formulate a measure of the reliability of the diagnostic algorithm, and then we discuss modifications of the diagnostic algorithm for the maximization of the reliability. The reliability of a diagnostic algorithm is measured by the amount of uncertainty consistent with no-failure of the diagnosis. Uncertainty is quantitatively represented with convex models.
Keywords: Robust reliability, convex models, Kalman filtering, multi-hypothesis diagnosis, rotating machinery, crack diagnosis
(24 pages, 1998)

4. F.-Th. Lentes, N. Siedow

Three-dimensional Radiative Heat Transfer in Glass Cooling Processes

For the numerical simulation of 3D radiative heat transfer in glasses and glass melts, practically applicable mathematical methods are needed to handle such problems optimal using workstation class computers. Since the exact solution would require super-computer capabilities we concentrate on approximate solutions with a high degree of accuracy. The following approaches are studied: 3D diffusion approximations and 3D ray-tracing methods.
(23 pages, 1998)

5. A. Klar, R. Wegener

A hierarchy of models for multilane vehicular traffic
Part I: Modeling

In the present paper multilane models for vehicular traffic are considered. A microscopic multilane model based on reaction thresholds is developed. Based on this model an Enskog like kinetic model is developed. In particular, care is taken to incorporate the correlations between the vehicles. From the kinetic model a fluid dynamic model is derived. The macroscopic coefficients are deduced from the underlying kinetic model. Numerical simulations are presented for all three levels of description in [10]. Moreover, a comparison of the results is given there.
(23 pages, 1998)

Part II: Numerical and stochastic investigations

In this paper the work presented in [6] is continued. The present paper contains detailed numerical investigations of the models developed there. A numerical method to treat the kinetic equations obtained in [6] are presented and results of the simulations are shown. Moreover, the stochastic correlation model used in [6] is described and investigated in more detail.
(17 pages, 1998)

6. A. Klar, N. Siedow

Boundary Layers and Domain Decomposition for Radiative Heat Transfer and Diffusion Equations: Applications to Glass Manufacturing Processes

In this paper domain decomposition methods for radiative transfer problems including conductive heat transfer are treated. The paper focuses on semi-transparent materials, like glass, and the associated conditions at the interface between the materials. Using asymptotic analysis we derive conditions for the coupling of the radiative transfer equations and a diffusion approximation. Several test cases are treated and a problem appearing in glass manufacturing processes is computed. The results clearly show the advantages of a domain decomposition approach. Accuracy equivalent to the solution of the global radiative transfer solution is achieved, whereas computation time is strongly reduced.
(24 pages, 1998)

7. I. Choquet

Heterogeneous catalysis modelling and numerical simulation in rarified gas flows Part I: Coverage locally at equilibrium

A new approach is proposed to model and simulate numerically heterogeneous catalysis in rarefied gas flows. It is developed to satisfy all together the following points:
1) describe the gas phase at the microscopic scale, as required in rarefied flows,
2) describe the wall at the macroscopic scale, to avoid prohibitive computational costs and consider not only crystalline but also amorphous surfaces,
3) reproduce on average macroscopic laws correlated with experimental results and
4) derive analytic models in a systematic and exact way. The problem is stated in the general framework of a non static flow in the vicinity of a catalytic and non porous surface (without aging). It is shown that the exact and systematic resolution method based on the Laplace transform, introduced previously by the author to model collisions in the gas phase, can be extended to the present problem. The proposed approach is applied to the modelling of the EleyRideal and LangmuirHinshelwood recombinations, assuming that the coverage is locally at equilibrium. The models are developed considering one atomic species and extended to the general case of several atomic species. Numerical calculations show that the models derived in this way reproduce with accuracy behaviors observed experimentally.
(24 pages, 1998)

8. J. Ohser, B. Steinbach, C. Lang

Efficient Texture Analysis of Binary Images

A new method of determining some characteristics of binary images is proposed based on a special linear filtering. This technique enables the estimation of the area fraction, the specific line length, and the specific integral of curvature. Furthermore, the specific length of the total projection is obtained, which gives detailed information about the texture of the image. The influence of lateral and directional resolution depending on the size of the applied filter mask is discussed in detail. The technique includes a method of increasing directional resolution for texture analysis while keeping lateral resolution as high as possible.
(17 pages, 1998)

9. J. Orlik

Homogenization for viscoelasticity of the integral type with aging and shrinkage

A multiphase composite with periodic distributed inclusions with a smooth boundary is considered in this contribution. The composite component materials are supposed to be linear viscoelastic and aging (of the non-convolution integral type, for which the Laplace transform with respect to time is not effectively applicable) and are subjected to isotropic shrinkage. The free shrinkage deformation can be considered as a fictitious temperature deformation in the behavior law. The procedure presented in this paper proposes a way to determine average (effective homogenized) viscoelastic and shrinkage (temperature) composite properties and the homogenized stressfield from known properties of the components. This is done by the extension of the asymptotic homogenization technique known for pure elastic nonhomogeneous bodies to the nonhomogeneous thermoviscoelasticity of the integral nonconvolution type. Up to now, the homogenization theory has not covered viscoelasticity of the integral type. SanchezPalencia (1980), Francfort & Suquet (1987) (see [2], [9]) have considered homogenization for viscoelasticity of the differential form and only up to the first derivative order. The integralmodeled viscoelasticity is more general then the differential one and includes almost all known differential models. The homogenization procedure is based on the construction of an asymptotic solution with respect to a period of the composite structure. This reduces the original problem to some auxiliary boundary value problems of elasticity and viscoelasticity on the unit periodic cell, of the same type as the original non-homogeneous problem. The existence and uniqueness results for such problems were obtained for kernels satisfying some constrain conditions. This is done by the extension of the Volterra integral operator theory to the Volterra operators with respect to the time, whose 1 kernels are space linear operators for any fixed time variables. Some ideas of such approach were proposed in [11] and [12], where the Volterra operators with kernels depending additionally on parameter were considered. This manuscript delivers results of the same nature for the case of the spaceoperator kernels.
(20 pages, 1998)

10. J. Mohring

Helmholtz Resonators with Large Aperture

The lowest resonant frequency of a cavity resonator is usually approximated by the classical Helmholtz formula. However, if the opening is rather large and the front wall is narrow this formula is no longer valid. Here we present a correction which is of third order in the ratio of the diameters of aperture and cavity. In addition to the high accuracy it allows to estimate the damping due to radiation. The result is found by applying the method of matched asymptotic expansions. The correction contains form factors describing the shapes of opening and cavity. They are computed for a number of standard geometries. Results are compared with numerical computations.
(21 pages, 1998)

11. H. W. Hamacher, A. Schöbel

On Center Cycles in Grid Graphs

Finding "good" cycles in graphs is a problem of great interest in graph theory as well as in locational analysis. We show that the center and median problems are NP hard in general graphs. This result holds both for the variable cardinality case (i.e. all cycles of the graph are considered) and the fixed cardinality case (i.e. only cycles with a given cardinality p are feasible). Hence it is of interest to investigate special cases where the problem is solvable in polynomial time. In grid graphs, the variable cardinality case is, for instance, trivially solvable if the shape of the cycle can be chosen freely. If the shape is fixed to be a rectangle one can analyze rectangles in grid graphs with, in sequence, fixed dimension, fixed cardinality, and variable cardinality. In all cases a complete characterization of the optimal cycles and closed form expressions of the optimal objective values are given, yielding polynomial time algorithms for all cases of center rectangle problems. Finally, it is shown that center cycles can be chosen as rectangles for small cardinalities such that the center cycle problem in grid graphs is in these cases completely solved.
(15 pages, 1998)

12. H. W. Hamacher, K.-H. Küfer

Inverse radiation therapy planning - a multiple objective optimisation approach

For some decades radiation therapy has been proved successful in cancer treatment. It is the major task of clinical radiation treatment planning to realize on the one hand a high level dose of radiation in the cancer tissue in order to obtain maximum tumor control. On the other hand it is obvious that it is absolutely necessary to keep in the tissue outside the tumor, particularly in organs at risk, the unavoidable radiation as low as possible.

No doubt, these two objectives of treatment planning - high level dose in the tumor, low radiation outside the tumor - have a basically contradictory nature. Therefore, it is no surprise that inverse mathematical models with dose distribution bounds tend to be infeasible in most cases. Thus, there is need for approximations compromising between overdosing the organs at risk and underdosing the target volume.

Differing from the currently used time consuming iterative approach, which measures deviation from an ideal (non-achievable) treatment plan using recursively trial-and-error weights for the organs of interest, we go a new way trying to avoid a priori weight choices and consider the treatment planning problem as a multiple objective linear programming problem: with each organ of interest, target tissue as well as organs at risk, we associate an objective function measuring the maximal deviation from the prescribed doses.

We build up a data base of relatively few efficient solutions representing and approximating the variety of Pareto solutions of the multiple objective linear programming problem. This data base can be easily scanned by physicians looking for an adequate treatment plan with the aid of an appropriate online tool.
(14 pages, 1999)

13. C. Lang, J. Ohser, R. Hilfer

On the Analysis of Spatial Binary Images

This paper deals with the characterization of microscopically heterogeneous, but macroscopically homogeneous spatial structures. A new method is presented which is strictly based on integral-geometric formulae such as Crofton's intersection formulae and Hadwiger's recursive definition of the Euler number. The corresponding algorithms have clear advantages over other techniques. As an example of application we consider the analysis of spatial digital images produced by means of Computer Assisted Tomography.
(20 pages, 1999)

14. M. Junk

On the Construction of Discrete Equilibrium Distributions for Kinetic Schemes

A general approach to the construction of discrete equilibrium distributions is presented. Such distribution functions can be used to set up Kinetic Schemes as well as Lattice Boltzmann methods. The general principles are also applied to the construction of Chapman Enskog distributions which are used in Kinetic Schemes for compressible Navier-Stokes equations.
(24 pages, 1999)

15. M. Junk, S. V. Raghurame Rao

A new discrete velocity method for Navier-Stokes equations

The relation between the Lattice Boltzmann Method, which has recently become popular, and the Kinetic Schemes, which are routinely used in Computational Fluid Dynamics, is explored. A new discrete velocity model for the numerical solution of Navier-Stokes equations for incompressible fluid flow is presented by combining both the approaches. The new scheme can be interpreted as a pseudo-compressibility method and, for a particular choice of parameters, this interpretation carries over to the Lattice Boltzmann Method.
(20 pages, 1999)

16. H. Neunzert

Mathematics as a Key to Key Technologies

The main part of this paper will consist of examples, how mathematics really helps to solve industrial problems; these examples are taken from our Institute for Industrial Mathematics, from research in the Technomathematics group at my university, but also from ECMI groups and a company called TecMath, which originated 10 years ago from my university group and has already a very successful history.
(39 pages (4 PDF-Files), 1999)

17. J. Ohser, K. Sandau

Considerations about the Estimation of the Size Distribution in Wicksell's Corpuscle Problem

Wicksell's corpuscle problem deals with the estimation of the size distribution of a population of particles, all having the same shape, using a lower dimensional sampling probe. This problem was originary formulated for particle systems occurring in life sciences but its solution is of actual and increasing interest in materials science. From a mathematical point of view, Wicksell's problem is an inverse problem where the interesting size distribution is the unknown part of a Volterra equation. The problem is often regarded ill-posed, because the structure of the integrand implies unstable numerical solutions. The accuracy of the numerical solutions is considered here using the condition number, which allows to compare different numerical methods with different (equidistant) class sizes and which indicates, as one result, that a finite section thickness of the probe reduces the numerical problems. Furthermore, the relative error of estimation is computed which can be split into two parts. One part consists of the relative discretization error that increases for increasing class size, and the second part is related to the relative statistical error which increases with decreasing class size. For both parts, upper bounds can be given and the sum of them indicates an optimal class width depending on some specific constants.
(18 pages, 1999)

18. E. Carrizosa, H. W. Hamacher, R. Klein, S. Nickel

Solving nonconvex planar location problems by finite dominating sets

It is well-known that some of the classical location problems with polyhedral gauges can be solved in polynomial time by finding a finite dominating set, i. e. a finite set of candidates guaranteed to contain at least one optimal location.

In this paper it is first established that this result holds for a much larger class of problems than currently considered in the literature. The model for which this result can be proven includes, for instance, location problems with attraction and repulsion, and location-allocation problems.

Next, it is shown that the approximation of general gauges by polyhedral ones in the objective function of our general model can be analyzed with regard to the subsequent error in the optimal objective value. For the approximation problem two different approaches are described, the sandwich procedure and the greedy algorithm. Both of these approaches lead - for fixed epsilon - to polynomial approximation algorithms with accuracy epsilon for solving the general model considered in this paper.

Keywords: Continuous Location, Polyhedral Gauges, Finite Dominating Sets, Approximation, Sandwich Algorithm, Greedy Algorithm
(19 pages, 2000)

19. A. Becker

A Review on Image Distortion Measures

Within this paper we review image distortion measures. A distortion measure is a criterion that assigns a "quality number" to an image. We distinguish between mathematical distortion measures and those distortion measures in-cooperating a priori knowledge about the imaging devices (e. g. satellite images), image processing algorithms or the human physiology. We will consider representative examples of different kinds of distortion measures and are going to discuss them.

Keywords: Distortion measure, human visual system
(26 pages, 2000)

20. H. W. Hamacher, M. Labbé, S. Nickel, T. Sonneborn

Polyhedral Properties of the Uncapacitated Multiple Allocation Hub Location Problem

We examine the feasibility polyhedron of the uncapacitated hub location problem (UHL) with multiple allocation, which has applications in the fields of air passenger and cargo transportation, telecommunication and postal delivery services. In particular we determine the dimension and derive some classes of facets of this polyhedron. We develop some general rules about lifting facets from the uncapacitated facility location (UFL) for UHL and projecting facets from UHL to UFL. By applying these rules we get a new class of facets for UHL which dominates the inequalities in the original formulation. Thus we get a new formulation of UHL whose constraints are all facet–defining. We show its superior computational performance by benchmarking it on a well known data set.

Keywords: integer programming, hub location, facility location, valid inequalities, facets, branch and cut
(21 pages, 2000)

21. H. W. Hamacher, A. Schöbel

Design of Zone Tariff Systems in Public Transportation

Given a public transportation system represented by its stops and direct connections between stops, we consider two problems dealing with the prices for the customers: The fare problem in which subsets of stops are already aggregated to zones and "good" tariffs have to be found in the existing zone system. Closed form solutions for the fare problem are presented for three objective functions. In the zone problem the design of the zones is part of the problem. This problem is NP hard and we therefore propose three heuristics which prove to be very successful in the redesign of one of Germany's transportation systems.
(30 pages, 2001)

22. D. Hietel, M. Junk, R. Keck, D. Teleaga

The Finite-Volume-Particle Method for Conservation Laws

In the Finite-Volume-Particle Method (FVPM), the weak formulation of a hyperbolic conservation law is discretized by restricting it to a discrete set of test functions. In contrast to the usual Finite-Volume approach, the test functions are not taken as characteristic functions of the control volumes in a spatial grid, but are chosen from a partition of unity with smooth and overlapping partition functions (the particles), which can even move along pre- scribed velocity fields. The information exchange between particles is based on standard numerical flux functions. Geometrical information, similar to the surface area of the cell faces in the Finite-Volume Method and the corresponding normal directions are given as integral quantities of the partition functions. After a brief derivation of the Finite-Volume-Particle Method, this work focuses on the role of the geometric coefficients in the scheme.
(16 pages, 2001)

23. T. Bender, H. Hennes, J. Kalcsics, M. T. Melo, S. Nickel

Location Software and Interface with GIS and Supply Chain Management

The objective of this paper is to bridge the gap between location theory and practice. To meet this objective focus is given to the development of software capable of addressing the different needs of a wide group of users. There is a very active community on location theory encompassing many research fields such as operations research, computer science, mathematics, engineering, geography, economics and marketing. As a result, people working on facility location problems have a very diverse background and also different needs regarding the software to solve these problems. For those interested in non-commercial applications (e. g. students and researchers), the library of location algorithms (LoLA can be of considerable assistance. LoLA contains a collection of efficient algorithms for solving planar, network and discrete facility location problems. In this paper, a detailed description of the functionality of LoLA is presented. In the fields of geography and marketing, for instance, solving facility location problems requires using large amounts of demographic data. Hence, members of these groups (e. g. urban planners and sales managers) often work with geographical information too s. To address the specific needs of these users, LoLA was inked to a geographical information system (GIS) and the details of the combined functionality are described in the paper. Finally, there is a wide group of practitioners who need to solve large problems and require special purpose software with a good data interface. Many of such users can be found, for example, in the area of supply chain management (SCM). Logistics activities involved in strategic SCM include, among others, facility location planning. In this paper, the development of a commercial location software tool is also described. The too is embedded in the Advanced Planner and Optimizer SCM software developed by SAP AG, Walldorf, Germany. The paper ends with some conclusions and an outlook to future activities.

Keywords: facility location, software development, geographical information systems, supply chain management

(48 pages, 2001)

24. H. W. Hamacher, S. A. Tjandra

Mathematical Modelling of Evacuation Problems: A State of Art

This paper details models and algorithms which can be applied to evacuation problems. While it concentrates on building evacuation many of the results are applicable also to regional evacuation. All models consider the time as main parameter, where the travel time between components of the building is part of the input and the overall evacuation time is the output. The paper distinguishes between macroscopic and microscopic evacuation models both of which are able to capture the evacuees' movement over time.

Macroscopic models are mainly used to produce good lower bounds for the evacuation time and do not consider any individual behavior during the emergency situation. These bounds can be used to analyze existing buildings or help in the design phase of planning a building. Macroscopic approaches which are based on dynamic network flow models (minimum cost dynamic flow, maximum dynamic flow, universal maximum flow, quickest path and quickest flow) are described. A special feature of the presented approach is the fact, that travel times of evacuees are not restricted to be constant, but may be density dependent. Using multicriteria optimization priority regions and blockage due to fire or smoke may be considered. It is shown how the modelling can be done using time parameter either as discrete or continuous parameter.

Microscopic models are able to model the individual evacuee's characteristics and the interaction among evacuees which influence their movement. Due to the corresponding huge amount of data one uses simulation approaches. Some probabilistic laws for individual evacuee's movement are presented. Moreover ideas to model the evacuee's movement using cellular automata (CA) and resulting software are presented.

In this paper we will focus on macroscopic models and only summarize some of the results of the microscopic approach. While most of the results are applicable to general evacuation situations, we concentrate on building evacuation.

(44 pages, 2001)

25. J. Kuhnert, S. Tiwari

Grid free method for solving the Poisson equation

A Grid free method for solving the Poisson equation is presented. This is an iterative method. The method is based on the weighted least squares approximation in which the Poisson equation is enforced to be satisfied in every iterations. The boundary conditions can also be enforced in the iteration process. This is a local approximation procedure. The Dirichlet, Neumann and mixed boundary value problems on a unit square are presented and the analytical solutions are compared with the exact solutions. Both solutions matched perfectly.

Keywords: Poisson equation, Least squares method, Grid free method

(19 pages, 2001)

26. T. Götz, H. Rave, D. Reinel-Bitzer, K. Steiner, H. Tiemeier

Simulation of the fiber spinning process

To simulate the influence of process parameters to the melt spinning process a fiber model is used and coupled with CFD calculations of the quench air flow. In the fiber model energy, momentum and mass balance are solved for the polymer mass flow. To calculate the quench air the Lattice Boltzmann method is used. Simulations and experiments for different process parameters and hole configurations are compared and show a good agreement.

Keywords: Melt spinning, fiber model, Lattice Boltzmann, CFD

(19 pages, 2001)

27. A. Zemitis

On interaction of a liquid film with an obstacle

In this paper mathematical models for liquid films generated by impinging jets are discussed. Attention is stressed to the interaction of the liquid film with some obstacle. S. G. Taylor [Proc. R. Soc. London Ser. A 253, 313 (1959)] found that the liquid film generated by impinging jets is very sensitive to properties of the wire which was used as an obstacle. The aim of this presentation is to propose a modification of the Taylor's model, which allows to simulate the film shape in cases, when the angle between jets is different from 180°. Numerical results obtained by discussed models give two different shapes of the liquid film similar as in Taylors experiments. These two shapes depend on the regime: either droplets are produced close to the obstacle or not. The difference between two regimes becomes larger if the angle between jets decreases. Existence of such two regimes can be very essential for some applications of impinging jets, if the generated liquid film can have a contact with obstacles.

Keywords: impinging jets, liquid film, models, numerical solution, shape

(22 pages, 2001)

28. I. Ginzburg, K. Steiner

Free surface lattice-Boltzmann method to model the filling of expanding cavities by Bingham Fluids

The filling process of viscoplastic metal alloys and plastics in expanding cavities is modelled using the lattice Boltzmann method in two and three dimensions. These models combine the regularized Bingham model for viscoplastic with a free-interface algorithm. The latter is based on a modified immiscible lattice Boltzmann model in which one species is the fluid and the other one is considered as vacuum. The boundary conditions at the curved liquid-vacuum interface are met without any geometrical front reconstruction from a first-order Chapman-Enskog expansion. The numerical results obtained with these models are found in good agreement with available theoretical and numerical analysis.

Keywords: Generalized LBE, free-surface phenomena, interface boundary conditions, filling processes, Bingham viscoplastic model, regularized models

(22 pages, 2001)

29. H. Neunzert

»Denn nichts ist für den Menschen als Menschen etwas wert, was er nicht mit Leidenschaft tun kann«
Vortrag anlässlich der Verleihung des Akademiepreises des Landes Rheinland-Pfalz am 21.11.2001

Was macht einen guten Hochschullehrer aus? Auf diese Frage gibt es sicher viele verschiedene, fachbezogene Antworten, aber auch ein paar allgemeine Gesichtspunkte: es bedarf der »Leidenschaft« für die Forschung (Max Weber), aus der dann auch die Begeisterung für die Lehre erwächst. Forschung und Lehre gehören zusammen, um die Wissenschaft als lebendiges Tun vermitteln zu können. Der Vortrag gibt Beispiele dafür, wie in angewandter Mathematik Forschungsaufgaben aus praktischen Alltagsproblemstellungen erwachsen, die in die Lehre auf verschiedenen Stufen (Gymnasium bis Graduiertenkolleg) einfließen; er leitet damit auch zu einem aktuellen Forschungsgebiet, der Mehrskalenanalyse mit ihren vielfältigen Anwendungen in Bildverarbeitung, Materialentwicklung und Strömungsmechanik über, was aber nur kurz gestreift wird. Mathematik erscheint hier als eine moderne Schlüsseltechnologie, die aber auch enge Beziehungen zu den Geistes- und Sozialwissenschaften hat.

Keywords: Lehre, Forschung, angewandte Mathematik, Mehrskalenanalyse, Strömungsmechanik

(18 pages, 2001)

30. J. Kuhnert, S. Tiwari

Finite pointset method based on the projection method for simulations of the incompressible Navier-Stokes equations

A Lagrangian particle scheme is applied to the projection method for the incompressible Navier-Stokes equations. The approximation of spatial derivatives is obtained by the weighted least squares method. The pressure Poisson equation is solved by a local iterative procedure with the help of the least squares method. Numerical tests are performed for two dimensional cases. The Couette flow, Poiseuelle flow, decaying shear flow and the driven cavity flow are presented. The numerical solutions are obtained for stationary as well as instationary cases and are compared with the analytical solutions for channel flows. Finally, the driven cavity in a unit square is considered and the stationary solution obtained from this scheme is compared with that from the finite element method.

Keywords: Incompressible Navier-Stokes equations, Meshfree method, Projection method, Particle scheme, Least squares approximation

AMS subject classification: 76D05, 76M28

(25 pages, 2001)

31. R. Korn, M. Krekel

Optimal Portfolios with Fixed Consumption or Income Streams

We consider some portfolio optimisation problems where either the investor has a desire for an a priori specified consumption stream or/and follows a deterministic pay in scheme while also trying to maximize expected utility from final wealth. We derive explicit closed form solutions for continuous and discrete monetary streams. The mathematical method used is classical stochastic control theory.

Keywords: Portfolio optimisation, stochastic control, HJB equation, discretisation of control problems.

(23 pages, 2002)

32. M. Krekel

Optimal portfolios with a loan dependent credit spread

If an investor borrows money he generally has to pay higher interest rates than he would have received, if he had put his funds on a savings account. The classical model of continuous time portfolio optimisation ignores this effect. Since there is obviously a connection between the default probability and the total

percentage of wealth, which the investor is in debt, we study portfolio optimisation with a control dependent interest rate. Assuming a logarithmic and a power utility function, respectively, we prove explicit formulae of the optimal control.
Keywords: Portfolio optimisation, stochastic control, HJB equation, credit spread, log utility, power utility, non-linear wealth dynamics
(25 pages, 2002)

33. J. Ohser, W. Nagel, K. Schladitz

The Euler number of discretized sets - on the choice of adjacency in homogeneous lattices

Two approaches for determining the Euler-Poincaré characteristic of a set observed on lattice points are considered in the context of image analysis { the integral geometric and the polyhedral approach. Information about the set is assumed to be available on lattice points only. In order to retain properties of the Euler number and to provide a good approximation of the true Euler number of the original set in the Euclidean space, the appropriate choice of adjacency in the lattice for the set and its background is crucial. Adjacencies are defined using tessellations of the whole space into polyhedrons. In R 3 , two new 14 adjacencies are introduced additionally to the well known 6 and 26 adjacencies. For the Euler number of a set and its complement, a consistency relation holds. Each of the pairs of adjacencies (14:1; 14:1), (14:2; 14:2), (6; 26), and (26; 6) is shown to be a pair of complementary adjacencies with respect to this relation. That is, the approximations of the Euler numbers are consistent if the set and its background (complement) are equipped with this pair of adjacencies. Furthermore, sufficient conditions for the correctness of the approximations of the Euler number are given. The analysis of selected microstructures and a simulation study illustrate how the estimated Euler number depends on the chosen adjacency. It also shows that there is not a uniquely best pair of adjacencies with respect to the estimation of the Euler number of a set in Euclidean space.
Keywords: image analysis, Euler number, neighborhod relationships, cuboidal lattice
(32 pages, 2002)

34. I. Ginzburg, K. Steiner

Lattice Boltzmann Model for Free-Surface flow and Its Application to Filling Process in Casting

A generalized lattice Boltzmann model to simulate free-surface is constructed in both two and three dimensions. The proposed model satisfies the interfacial boundary conditions accurately. A distinctive feature of the model is that the collision processes is carried out only on the points occupied partially or fully by the fluid. To maintain a sharp interfacial front, the method includes an anti-diffusion algorithm. The unknown distribution functions at the interfacial region are constructed according to the first order Chapman-Enskog analysis. The interfacial boundary conditions are satisfied exactly by the coefficients in the Chapman-Enskog expansion. The distribution functions are naturally expressed in the local interfacial coordinates. The macroscopic quantities at the interface are extracted from the least-square solutions of a locally linearized system obtained from the known distribution functions. The proposed method does not require any geometric front construction and is robust for any interfacial topology. Simulation results of realistic filling process are presented: rectangular cavity in two dimensions and Hammer box, Campbell box, Sheffield box, and Motorblock in three dimensions. To enhance the stability at high Reynolds numbers, various upwind-type schemes are developed. Free-slip and no-slip boundary conditions are also discussed.
Keywords: Lattice Boltzmann models; free-surface phenomena; interface boundary conditions; filling processes; injection molding; volume of fluid method; interface boundary conditions; advection-schemes; upwind-schemes
(54 pages, 2002)

35. M. Günther, A. Klar, T. Materne, R. Wegener

Multivalued fundamental diagrams and stop and go waves for continuum traffic equations

In the present paper a kinetic model for vehicular traffic leading to multivalued fundamental diagrams is developed and investigated in detail. For this model phase transitions can appear depending on the local density and velocity of the flow. A derivation of associated macroscopic traffic equations from the kinetic equation is given. Moreover, numerical experiments show the appearance of stop and go waves for highway traffic with a bottleneck.
Keywords: traffic flow, macroscopic equations, kinetic derivation, multivalued fundamental diagram, stop and go waves, phase transitions
(25 pages, 2002)

36. S. Feldmann, P. Lang, D. Prätzel-Wolters

Parameter influence on the zeros of network determinants

To a network N(q) with determinant D(s;q) depending on a parameter vector q Î Rr via identification of some of its vertices, a network N^ (q) is assigned. The paper deals with procedures to find N^ (q), such that its determinant D^ (s;q) admits a factorization in the determinants of appropriate subnetworks, and with the estimation of the deviation of the zeros of D^ from the zeros of D. To solve the estimation problem state space methods are applied.
Keywords: Networks, Equicofactor matrix polynomials, Realization theory, Matrix perturbation theory
(30 pages, 2002)

37. K. Koch, J. Ohser, K. Schladitz

Spectral theory for random closed sets and estimating the covariance via frequency space

A spectral theory for stationary random closed sets is developed and provided with a sound mathematical basis. Definition and proof of existence of the Bartlett spectrum of a stationary random closed set as well as the proof of a Wiener-Khintchine theorem for the power spectrum are used to two ends: First, well known second order characteristics like the covariance can be estimated faster than usual via frequency space. Second, the Bartlett spectrum and the power spectrum can be used as second order characteristics in frequency space. Examples show, that in some cases information about the random closed set is easier to obtain from these characteristics in frequency space than from their real world counterparts.
Keywords: Random set, Bartlett spectrum, fast Fourier transform, power spectrum
(28 pages, 2002)

38. D. d'Humières, I. Ginzburg

Multi-reflection boundary conditions for lattice Boltzmann models

We present a unified approach of several boundary conditions for lattice Boltzmann models. Its general framework is a generalization of previously introduced schemes such as the bounce-back rule, linear or quadratic interpolations, etc. The objectives are two fold: first to give theoretical tools to study the existing boundary conditions and their corresponding accuracy; secondly to design formally third- order accurate boundary conditions for general flows. Using these boundary conditions, Couette and Poiseuille flows are exact solution of the lattice Boltzmann models for a Reynolds number Re = 0 (Stokes limit).
Numerical comparisons are given for Stokes flows in periodic arrays of spheres and cylinders, linear periodic array of cylinders between moving plates and for Navier-Stokes flows in periodic arrays of cylinders for Re < 200. These results show a significant improvement of the overall accuracy when using the linear interpolations instead of the bounce-back reflection (up to an order of magnitude on the hydrodynamics fields). Further improvement is achieved with the new multi-reflection boundary conditions, reaching a level of accuracy close to the quasi-analytical reference solutions, even for rather modest grid resolutions and few points in the narrowest channels. More important, the pressure and velocity fields in the vicinity of the obstacles are much smoother with multi-reflection than with the other boundary conditions.
Finally the good stability of these schemes is highlighted by some simulations of moving obstacles: a cylinder between flat walls and a sphere in a cylinder.
Keywords: lattice Boltzmann equation, boudary condistions, bounce-back rule, Navier-Stokes equation
(72 pages, 2002)

39. R. Korn

Elementare Finanzmathematik

Im Rahmen dieser Arbeit soll eine elementar gehaltene Einführung in die Aufgabenstellungen und Prinzipien der modernen Finanzmathematik gegeben werden. Insbesondere werden die Grundlagen der Modellierung von Aktienkursen, der Bewertung von Optionen und der Portfolio-Optimierung vorgestellt. Natürlich können die verwendeten Methoden und die entwickelte Theorie nicht in voller Allgemeinheit für den Schulunterricht verwendet werden, doch sollen einzelne Prinzipien so heraus gearbeitet werden, dass sie auch an einfachen Beispielen verstanden werden können.
Keywords: Finanzmathematik, Aktien, Optionen, Portfolio-Optimierung, Börse, Lehrerweiterbildung, Mathematikunterricht
(98 pages, 2002)

40. J. Kallrath, M. C. Müller, S. Nickel

Batch Presorting Problems: Models and Complexity Results

In this paper we consider short term storage systems. We analyze presorting strategies to improve the effiency of these storage systems. The presorting task is called Batch PreSorting Problem (BPSP). The BPSP is a variation of an assigment problem, i. e., it has an assigment problem kernel and some additional constraints. We present different types of these presorting problems, introduce mathematical programming formulations and prove the NP-completeness for one type of the BPSP. Experiments are carried out in order to compare the different model formulations and to investigate the behavior of these models.
Keywords: Complexity theory, Integer programming, Assigment, Logistics
(19 pages, 2002)

41. J. Linn

On the frame-invariant description of the phase space of the Folgar-Tucker equation

The Folgar-Tucker equation is used in flow simulations of fiber suspensions to predict fiber orientation depending on the local flow. In this paper, a complete, frame-invariant description of the phase space of this differential equation is presented for the first time.
Key words: fiber orientation, Folgar-Tucker equation, injection molding
(5 pages, 2003)

42. T. Hanne, S. Nickel

A Multi-Objective Evolutionary Algorithm for Scheduling and Inspection Planning in Software Development Projects

In this article, we consider the problem of planning inspections and other tasks within a software development (SD) project with respect to the objectives quality (no. of defects), project duration, and costs. Based on a discrete-event simulation model of SD processes comprising the phases coding, inspection, test, and rework, we present a simplified formulation of the problem as a multiobjective optimization problem. For solving the problem (i. e. finding an approximation of the efficient set) we develop a multiobjective evolutionary algorithm. Details of the algorithm are discussed as well as results of its application to sample problems.
Key words: multiple objective programming, project management and scheduling, software development, evolutionary algorithms, efficient set
(29 pages, 2003)

43. T. Bortfeld , K.-H. Küfer, M. Monz, A. Scherrer, C. Thieke, H. Trinkaus

Intensity-Modulated Radiotherapy - A Large Scale Multi-Criteria Programming Problem -

Radiation therapy planning is always a tight rope walk between dangerous insufficient dose in the target volume and life threatening overdosing of organs at risk. Finding ideal balances between these inherently contradictory goals challenges dosimetrists and physicians in their daily practice. Today's planning systems are typically based on a single evaluation function that measures the quality of a radiation treatment plan. Unfortunately, such a one dimensional approach cannot satisfactorily map the different backgrounds of physicians and the patient dependent necessities. So, too often a time consuming iteration process between evaluation of dose distribution and redefinition of the evaluation function is needed.
In this paper we propose a generic multi-criteria approach based on Pareto's solution concept. For each entity of interest - target volume or organ at risk a structure dependent evaluation function is defined measuring deviations from ideal doses that are calculated from statistical functions. A reasonable bunch of clinically meaningful Pareto optimal solutions are stored in a data base, which can be interactively searched by physicians. The system guarantees dynamical planning as well as the discussion of tradeoffs between different entities.
Mathematically, we model the upcoming inverse problem as a multi-criteria linear programming problem. Because of the large scale nature of the problem it is not possible to solve the problem in a 3D-setting without adaptive reduction by appropriate approximation schemes.
Our approach is twofold: First, the discretization of the continuous problem is based on an adaptive hierarchical clustering process which is used for a local refinement of constraints during the optimization procedure. Second, the set of Pareto optimal solutions is approximated by an adaptive grid of representatives that are found by a hybrid process of calculating extreme compromises and interpolation methods.
Keywords: multiple criteria optimization, representative systems of Pareto solutions, adaptive triangulation, clustering and disaggregation techniques, visualization of Pareto solutions, medical physics, external beam radiotherapy planning, intensity modulated radiotherapy
(31 pages, 2003)

44. T. Halfmann, T. Wichmann

Overview of Symbolic Methods in Industrial Analog Circuit Design

Industrial analog circuits are usually designed using numerical simulation tools. To obtain a deeper circuit understanding, symbolic analysis techniques can additionally be applied. Approximation methods which reduce the complexity of symbolic expressions are needed in order to handle industrial-sized problems. This paper will give an overview to the field of symbolic analog circuit analysis. Starting with a motivation, the state-of-the-art simplification algorithms for linear as well as for nonlinear circuits are presented. The basic ideas behind the different techniques are described, whereas the technical details can be found in the cited references. Finally, the application of linear and nonlinear symbolic analysis will be shown on two example circuits.
Keywords: CAD, automated analog circuit design, symbolic analysis, computer algebra, behavioral modeling, system simulation, circuit sizing, macro modeling, differential-algebraic equations, index
(17 pages, 2003)

45. S. E. Mikhailov, J. Orlik

Asymptotic Homogenisation in Strength and Fatigue Durability Analysis of Composites

Asymptotic homogenisation technique and two-scale convergence is used for analysis of macro-strength and fatigue durability of composites with a periodic structure under cyclic loading. The linear damage accumulation rule is employed in the phenomenological micro-durability conditions (for each component of the composite) under varying cyclic loading. Both local and non-local strength and durability conditions are analysed. The strong convergence of the strength and fatigue damage measure as the structure period tends to zero is proved and their limiting values are estimated.
Keywords: multiscale structures, asymptotic homogenization, strength, fatigue, singularity, non-local conditions
(14 pages, 2003)

46. P. Domínguez-Marín, P. Hansen, N. Mladenovi´c , S. Nickel

Heuristic Procedures for Solving the Discrete Ordered Median Problem

We present two heuristic methods for solving the Discrete Ordered Median Problem (DOMP), for which no such approaches have been developed so far. The DOMP generalizes classical discrete facility location problems, such as the p-median, p-center and Uncapacitated Facility Location problems. The first procedure proposed in this paper is based on a genetic algorithm developed by Moreno Vega [MV96] for p-median and p-center problems. Additionally, a second heuristic approach based on the Variable Neighborhood Search metaheuristic (VNS) proposed by Hansen & Mladenovic [HM97] for the p-median problem is described. An extensive numerical study is presented to show the efficiency of both heuristics and compare them.
Keywords: genetic algorithms, variable neighborhood search, discrete facility location
(31 pages, 2003)

47. N. Boland, P. Domínguez-Marín, S. Nickel, J. Puerto

Exact Procedures for Solving the Discrete Ordered Median Problem

The Discrete Ordered Median Problem (DOMP) generalizes classical discrete location problems, such as the N-median, N-center and Uncapacitated Facility Location problems. It was introduced by Nickel [16], who formulated it as both a nonlinear and a linear integer program. We propose an alternative integer linear programming formulation for the DOMP, discuss relationships between both integer linear programming formulations, and show how properties of optimal solutions can be used to strengthen these formulations. Moreover, we present a specific branch and bound procedure to solve the DOMP more efficiently. We test the integer linear programming formulations and this branch and bound method computationally on randomly generated test problems.
Keywords: discrete location, Integer programming
(41 pages, 2003)

48. S. Feldmann, P. Lang

Padé-like reduction of stable discrete linear systems preserving their stability

A new stability preserving model reduction algorithm for discrete linear SISO-systems based on their impulse response is proposed. Similar to the Padé approximation, an equation system for the Markov parameters involving the Hankel matrix is considered, that here however is chosen to be of very high dimension. Although this equation system therefore in general cannot be solved exactly, it is proved that the approximate solution, computed via the Moore-Penrose inverse, gives rise to a stability preserving reduction scheme, a property that cannot be guaranteed for the Padé approach. Furthermore, the proposed algorithm is compared to another stability preserving reduction approach, namely the balanced truncation method, showing comparable performance of the reduced systems. The balanced truncation method however starts from a state space description of the systems and in general is expected to be more computational demanding.
Keywords: Discrete linear systems, model reduction, stability, Hankel matrix, Stein equation
(16 pages, 2003)

49. J. Kallrath, S. Nickel

A Polynomial Case of the Batch Presorting Problem

This paper presents new theoretical results for a special case of the batch presorting problem (BPSP). We will show tht this case can be solved in polynomial time. Offline and online algorithms are presented for solving the BPSP. Competetive analysis is used for comparing the algorithms.
Keywords: batch presorting problem, online optimization, competetive analysis, polynomial algorithms, logistics
(17 pages, 2003)

50. T. Hanne, H. L. Trinkaus

knowCube for MCDM – Visual and Interactive Support for Multicriteria Decision Making

In this paper, we present a novel multicriteria decision support system (MCDSS), called knowCube, consisting of components for knowledge organization, generation, and navigation. Knowledge organization rests upon a database for managing qualitative and quantitative criteria, together with add-on information. Knowledge generation serves filling the database via e. g. identification, optimization, classification or simulation. For "finding needles in haycocks", the knowledge navigation component supports graphical database retrieval and interactive, goal-oriented problem solving. Navigation "helpers" are, for instance, cascading criteria aggregations, modifiable metrics, ergonomic interfaces, and customizable visualizations. Examples from real-life projects, e.g. in industrial engineering and in the life sciences, illustrate the application of our MCDSS.
Key words: Multicriteria decision making, knowledge management, decision support systems, visual interfaces, interactive navigation, real-life applications.
(26 pages, 2003)

51. O. Iliev, V. Laptev

On Numerical Simulation of Flow Through Oil Filters

This paper concerns numerical simulation of flow through oil filters. Oil filters consist of filter housing (filter box), and a porous filtering medium, which completely separates the inlet from the outlet. We discuss mathematical models, describing coupled flows in the pure liquid subregions and in the porous filter media, as well as interface conditions between them. Further, we reformulate the problem in fictitious regions method manner, and discuss peculiarities of the numerical algorithm in solving the coupled system. Next, we show numerical results, validating the model and the algorithm. Finally, we present results from simulation of 3-D oil flow through a real car filter.
Keywords: oil filters, coupled flow in plain and porous media, Navier-Stokes, Brinkman, numerical simulation
(8 pages, 2003)

52. W. Dörfler, O. Iliev, D. Stoyanov, D. Vassileva

On a Multigrid Adaptive Refinement Solver for Saturated Non-Newtonian Flow in Porous Media

A multigrid adaptive refinement algorithm for non-Newtonian flow in porous media is presented. The saturated flow of a non-Newtonian fluid is described by the continuity equation and the generalized Darcy law. The resulting second order nonlinear elliptic equation is discretized by a finite volume method on a cell-centered grid. A nonlinear full-multigrid, full-approximation-storage algorithm is implemented. As a smoother, a single grid solver based on Picard linearization and Gauss-Seidel relaxation is used. Further, a local refinement multigrid algorithm on a composite grid is developed. A residual based error indicator is used in the adaptive refinement criterion. A special implementation approach is used, which allows us to perform unstructured local refinement in conjunction with the finite volume discretization. Several results from numerical experiments are presented in order to examine the performance of the solver.
Keywords: Nonlinear multigrid, adaptive refinement, non-Newtonian flow in porous media
(17 pages, 2003)

53. S. Kruse

On the Pricing of Forward Starting Options under Stochastic Volatility

We consider the problem of pricing European forward starting options in the presence of stochastic volatility. By performing a change of measure using the asset price at the time of strike determination as a numeraire, we derive a closed-form solution based on Heston's model of stochastic volatility.

Keywords: Option pricing, forward starting options, Heston model, stochastic volatility, cliquet options

(11 pages, 2003)

54. O. Iliev, D. Stoyanov

Multigrid – adaptive local refinement solver for incompressible flows

A non-linear multigrid solver for incompressible Navier-Stokes equations, exploiting finite volume discretization of the equations, is extended by adaptive local refinement. The multigrid is the outer iterative cycle, while the SIMPLE algorithm is used as a smoothing procedure. Error indicators are used to define the refinement subdomain. A special implementation approach is used, which allows to perform unstructured local refinement in conjunction with the finite volume discretization. The multigrid - adaptive local refinement algorithm is tested on 2D Poisson equation and further is applied to a lid-driven flows in a cavity (2D and 3D case), comparing the results with bench-mark data. The software design principles of the solver are also discussed.

Keywords: Navier-Stokes equations, incompressible flow, projection-type splitting, SIMPLE, multigrid methods, adaptive local refinement, lid-driven flow in a cavity

(37 pages, 2003)

55. V. Starikovicius

The multiphase flow and heat transfer in porous media

In first part of this work, summaries of traditional Multiphase Flow Model and more recent Multiphase Mixture Model are presented. Attention is being paid to attempts include various heterogeneous aspects into models. In second part, MMM based differential model for two-phase immiscible flow in porous media is considered. A numerical scheme based on the sequential solution procedure and control volume based finite difference schemes for the pressure and saturation-conservation equations is developed. A computer simulator is built, which exploits object-oriented programming techniques. Numerical result for several test problems are reported.

Keywords: Two-phase flow in porous media, various formulations, global pressure, multiphase mixture model, numerical simulation

(30 pages, 2003)

56. P. Lang, A. Sarishvili, A. Wirsen

Blocked neural networks for knowledge extraction in the software development process

One of the main goals of an organization developing software is to increase the quality of the software while at the same time to decrease the costs and the duration of the development process. To achieve this, various decisions e.ecting this goal before and during the development process have to be made by the managers. One appropriate tool for decision support are simulation models of the software life cycle, which also help to understand the dynamics of the software development process. Building up a simulation model requires a mathematical description of the interactions between di.erent objects involved in the development process. Based on experimental data, techniques from the .eld of knowledge discovery can be used to quantify these interactions and to generate new process knowledge based on the analysis of the determined relationships. In this paper blocked neuronal networks and related relevance measures will be presented as an appropriate tool for quanti.cation and validation of qualitatively known dependencies in the software development process.

Keywords: Blocked Neural Networks, Nonlinear Regression, Knowledge Extraction, Code Inspection

(21 pages, 2003)

57. H. Knaf, P. Lang, S. Zeiser

Diagnosis aiding in Regulation Thermography using Fuzzy Logic

The objective of the present article is to give an overview of an application of Fuzzy Logic in Regulation Thermography, a method of medical diagnosis support. An introduction to this method of the complementary medical science based on temperature measurements – so-called thermograms – is provided. The process of modelling the physician's thermogram evaluation rules using the calculus of Fuzzy Logic is explained.

Keywords: fuzzy logic,knowledge representation, expert system

(22 pages, 2003)

58. M.T. Melo, S. Nickel, F. Saldanha da Gama

Largescale models for dynamic multi-commodity capacitated facility location

In this paper we focus on the strategic design of supply chain networks. We propose a mathematical modeling framework that captures many practical aspects of network design problems simultaneously but which have not received adequate attention in the literature. The aspects considered include: dynamic planning horizon, generic supply chain network structure, external supply of materials, inventory opportunities for goods, distribution of commodities, facility configuration, availability of capital for investments, and storage limitations. Moreover, network configuration decisions concerning the gradual relocation of facilities over the planning horizon are considered. To cope with fluctuating demands, capacity expansion and reduction scenarios are also analyzed as well as modular capacity shifts. The relation of the proposed modeling framework with existing models is discussed. For problems of reasonable size we report on our computational experience with standard mathematical programming software. In particular, useful insights on the impact of various factors on network design decisions are provided.

Keywords: supply chain management, strategic planning, dynamic location, modeling

(40 pages, 2003)

59. J. Orlik

Homogenization for contact problems with periodically rough surfaces

We consider the contact of two elastic bodies with rough surfaces at the interface. The size of the micro-peaks and valleys is very small compared with the macrosize of the bodies' domains. This makes the direct application of the FEM for the calculation of the contact problem prohibitively costly. A method is developed that allows deriving a macrocontact condition on the interface. The method involves the twoscale asymptotic homogenization procedure that takes into account the microgeometry of the interface layer and the stiffnesses of materials of both domains. The macrocontact condition can then be used in a FEM model for the contact problem on the macrolevel. The averaged contact stiffness obtained allows the replacement of the interface layer in the macromodel by the macrocontact condition.

Keywords: asymptotic homogenization, contact problems

(28 pages, 2004)

60. A. Scherrer, K.-H. Küfer, M. Monz, F. Alonso, T. Bortfeld

IMRT planning on adaptive volume structures – a significant advance of computational complexity

In intensity-modulated radiotherapy (IMRT) planning the oncologist faces the challenging task of finding a treatment plan that he considers to be an ideal compromise of the inherently contradictive goals of delivering a sufficiently high dose to the target while widely sparing critical structures. The search for this a priori unknown compromise typically requires the computation of several plans, i.e. the solution of several optimization problems. This accumulates to a high computational expense due to the large scale of these problems - a consequence of the discrete problem formulation. This paper presents the adaptive clustering method as a new algorithmic concept to overcome these difficulties. The computations are performed on an individually adapted structure of voxel clusters rather than on the original voxels leading to a decisively reduced computational complexity as numerical examples on real clinical data demonstrate. In contrast to many other similar concepts, the typical trade-off between a reduction in computational complexity and a loss in exactness can be avoided: the adaptive clustering method produces the optimum of the original problem. This flexible method can be applied to both single- and multi-criteria optimization methods based on most of the convex evaluation functions used in practice.

Keywords: Intensity-modulated radiation therapy (IMRT), inverse treatment planning, adaptive volume structures, hierarchical clustering, local refinement, adaptive clustering, convex programming, mesh generation, multi-grid methods

(24 pages, 2004)

61. D. Kehrwald

Parallel lattice Boltzmann simulation of complex flows

After a short introduction to the basic ideas of lattice Boltzmann methods and a brief description of a modern parallel computer, it is shown how lattice Boltzmann schemes are successfully applied for simulating fluid flow in microstructures and calculating material properties of porous media. It is explained how lattice Boltzmann schemes compute the gradient of the velocity field without numerical differentiation. This feature is then utilised for the simulation of pseudo-plastic fluids, and numerical results are presented for a simple benchmark problem as well as for the simulation of liquid composite moulding.

Keywords: Lattice Boltzmann methods, parallel computing, microstructure simulation, virtual material design, pseudo-plastic fluids, liquid composite moulding

(12 pages, 2004)

62. O. Iliev, J. Linn, M. Moog, D. Niedziela, V. Starikovicius

On the Performance of Certain Iterative Solvers for Coupled Systems Arising in Discretization of Non-Newtonian Flow Equations

Iterative solution of large scale systems arising after discretization and linearization of the unsteady non-Newtonian Navier–Stokes equations is studied. cross WLF model is used to account for the non-Newtonian behavior of the fluid. Finite volume method is used to discretize the governing system of PDEs. Viscosity is treated explicitely (e.g., it is taken from the previous time step), while other terms are treated implicitly. Different preconditioners (block–diagonal, block–triangular, relaxed incomplete LU factorization, etc.) are used in conjunction with advanced iterative methods, namely, BiCGStab, CGS, GMRES. The action of the preconditioner in fact requires inverting different blocks. For this purpose, in addition to preconditioned BiCGStab, CGS, GMRES, we use also algebraic multigrid method (AMG). The performance of the iterative solvers is studied with respect to the number of unknowns, characteristic velocity in the basic flow, time step, deviation from Newtonian behavior, etc. Results from numerical experiments are presented and discussed.

Keywords: Performance of iterative solvers, Preconditioners, Non-Newtonian flow

(17 pages, 2004)

63. R. Ciegis, O. Iliev, S. Rief, K. Steiner

On Modelling and Simulation of Different Regimes for Liquid Polymer Moulding

In this paper we consider numerical algorithms for solving a system of nonlinear PDEs arising in modeling of liquid polymer injection. We investigate the particular case when a porous preform is located within the mould, so that the liquid polymer flows through a porous medium during the filling stage. The nonlinearity of the governing system of PDEs is due to the non-Newtonian behavior of the polymer, as well as due to the moving free boundary. The latter is related to the penetration front and a Stefan type problem is formulated to account for it. A finite-volume method is used

to approximate the given differential problem. Results of numerical experiments are presented.
We also solve an inverse problem and present algorithms for the determination of the absolute preform permeability coefficient in the case when the velocity of the penetration front is known from measurements. In both cases (direct and inverse problems) we emphasize on the specifics related to the non-Newtonian behavior of the polymer. For completeness, we discuss also the Newtonian case. Results of some experimental measurements are presented and discussed.
Keywords: Liquid Polymer Moulding, Modelling, Simulation, Infiltration, Front Propagation, non-Newtonian flow in porous media
(43 pages, 2004)

64. T. Hanne, H. Neu

Simulating Human Resources in Software Development Processes

In this paper, we discuss approaches related to the explicit modeling of human beings in software development processes. While in most older simulation models of software development processes, esp. those of the system dynamics type, humans are only represented as a labor pool, more recent models of the discrete-event simulation type require representations of individual humans. In that case, particularities regarding the person become more relevant. These individual effects are either considered as stochastic variations of productivity, or an explanation is sought based on individual characteristics, such as skills for instance. In this paper, we explore such possibilities by recurring to some basic results in psychology, sociology, and labor science. Various specific models for representing human effects in software process simulation are discussed.
Keywords: Human resource modeling, software process, productivity, human factors, learning curve
(14 pages, 2004)

65. O. Iliev, A. Mikelic, P. Popov

Fluid structure interaction problems in deformable porous media: Toward permeability of deformable porous media

In this work the problem of fluid flow in deformable porous media is studied. First, the stationary fluid-structure interaction (FSI) problem is formulated in terms of incompressible Newtonian fluid and a linearized elastic solid. The flow is assumed to be characterized by very low Reynolds number and is described by the Stokes equations. The strains in the solid are small allowing for the solid to be described by the Lame equations, but no restrictions are applied on the magnitude of the displacements leading to strongly coupled, nonlinear fluid-structure problem. The FSI problem is then solved numerically by an iterative procedure which solves sequentially fluid and solid subproblems. Each of the two subproblems is discretized by finite elements and the fluid-structure coupling is reduced to an interface boundary condition. Several numerical examples are presented and the results from the numerical computations are used to perform permeability computations for different geometries.
Keywords: fluid-structure interaction, deformable porous media, upscaling, linear elasticity, stokes, finite elements
(23 pages, 2004)

66. F. Gaspar, O. Iliev, F. Lisbona, A. Naumovich, P. Vabishchevich

On numerical solution of 1-D poroelasticity equations in a multilayered domain

Finite volume discretization of Biot system of poroelasticity in a multilayered domain is presented. Staggered grid is used in order to avoid nonphysical oscillations of the numerical solution, appearing when a collocated grid is used. Various numerical experiments are presented in order to illustrate the accuracy of the finite difference scheme. In the first group of experiments, problems having analytical solutions are solved, and the order of convergence for the velocity, the pressure, the displacements, and the stresses is analyzed. In the second group of experiments numerical solution of real problems is presented.
Keywords: poroelasticity, multilayered material, finite volume discretization, MAC type grid
(41 pages, 2004)

67. J. Ohser, K. Schladitz, K. Koch, M. Nöthe

Diffraction by image processing and its application in materials science

A spectral theory for constituents of macroscopically homogeneous random microstructures modeled as homogeneous random closed sets is developed and provided with a sound mathematical basis, where the spectrum obtained by Fourier methods corresponds to the angular intensity distribution of x-rays scattered by this constituent. It is shown that the fast Fourier transform applied to three-dimensional images of microstructures obtained by micro-tomography is a powerful tool of image processing. The applicability of this technique is is demonstrated in the analysis of images of porous media.
Keywords: porous microstructure, image analysis, random set, fast Fourier transform, power spectrum, Bartlett spectrum
(13 pages, 2004)

68. H. Neunzert

Mathematics as a Technology: Challenges for the next 10 Years

No doubt: Mathematics has become a technology in its own right, maybe even a key technology. Technology may be defined as the application of science to the problems of commerce and industry. And science? Science maybe defined as developing, testing and improving models for the prediction of system behavior; the language used to describe these models is mathematics and mathematics provides methods to evaluate these models. Here we are! Why has mathematics become a technology only recently? Since it got a tool, a tool to evaluate complex, "near to reality" models: Computer! The model may be quite old – Navier-Stokes equations describe flow behavior rather well, but to solve these equations for realistic geometry and higher Reynolds numbers with sufficient precision is even for powerful parallel computing a real challenge. Make the models as simple as possible, as complex as necessary – and then evaluate them with the help of efficient and reliable algorithms: These are genuine mathematical tasks.
Keywords: applied mathematics, technology, modelling, simulation, visualization, optimization, glass processing, spinning processes, fiber-fluid interaction, trubulence effects, topological optimization, multicriteria optimization, Uncertainty and Risk, financial mathematics, Malliavin calculus, Monte-Carlo methods, virtual material design, filtration, bio-informatics, system biology
(29 pages, 2004)

69. R. Ewing, O. Iliev, R. Lazarov, A. Naumovich

On convergence of certain finite difference discretizations for 1D poroelasticity interface problems

Finite difference discretizations of 1D poroelasticity equations with discontinuous coefficients are analyzed. A recently suggested FD discretization of poroelasticity equations with constant coefficients on staggered grid, [5], is used as a basis. A careful treatment of the interfaces leads to harmonic averaging of the discontinuous coefficients. Here, convergence for the pressure and for the displacement is proven in certain norms for the scheme with harmonic averaging (HA). Order of convergence 1.5 is proven for arbitrary located interface, and second order convergence is proven for the case when the interface coincides with a grid node. Furthermore, following the ideas from [3], modified HA discretization are suggested for particular cases. The velocity and the stress are approximated with second order on the interface in this case. It is shown that for wide class of problems, the modified discretization provides better accuracy. Second order convergence for modified scheme is proven for the case when the interface coincides with a displacement grid node. Numerical experiments are presented in order to illustrate our considerations.
Keywords: poroelasticity, multilayered material, finite volume discretizations, MAC type grid, error estimates
(26 pages,2004)

70. W. Dörfler, O. Iliev, D. Stoyanov, D. Vassileva

On Efficient Simulation of Non-Newtonian Flow in Saturated Porous Media with a Multigrid Adaptive Refinement Solver

Flow of non-Newtonian in saturated porous media can be described by the continuity equation and the generalized Darcy law. Efficient solution of the resulting second order nonlinear elliptic equation is discussed here. The equation is discretized by a finite volume method on a cell-centered grid. Local adaptive refinement of the grid is introduced in order to reduce the number of unknowns. A special implementation approach is used, which allows us to perform unstructured local refinement in conjunction with the finite volume discretization. Two residual based error indicators are exploited in the adaptive refinement criterion. Second order accurate discretization on the interfaces between refined and non-refined subdomains, as well as on the boundaries with Dirichlet boundary condition, are presented here, as an essential part of the accurate and efficient algorithm. A nonlinear full approximation storage multigrid algorithm is developed especially for the above described composite (coarse plus locally refined) grid approach. In particular, second order approximation around interfaces is a result of a quadratic approximation of slave nodes in the multigrid - adaptive refinement (MG-AR) algorithm. Results from numerical solution of various academic and practice-induced problems are presented and the performance of the solver is discussed.
Keywords: Nonlinear multigrid, adaptive renement, non-Newtonian in porous media
(25 pages, 2004)

71. J. Kalcsics, S. Nickel, M. Schröder

Towards a Unified Territory Design Approach – Applications, Algorithms and GIS Integration

Territory design may be viewed as the problem of grouping small geographic areas into larger geographic clusters called territories in such a way that the latter are acceptable according to relevant planning criteria. In this paper we review the existing literature for applications of territory design problems and solution approaches for solving these types of problems. After identifying features common to all applications we introduce a basic territory design model and present in detail two approaches for solving this model: a classical location–allocation approach combined with optimal split resolution techniques and a newly developed computational geometry based method. We present computational results indicating the efficiency and suitability of the latter method for solving large–scale practical problems in an interactive environment. Furthermore, we discuss extensions to the basic model and its integration into Geographic Information Systems.
Keywords: territory desgin, political districting, sales territory alignment, optimization algorithms, Geographical Information Systems
(40 pages, 2005)

72. K. Schladitz, S. Peters, D. Reinel-Bitzer, A. Wiegmann, J. Ohser

Design of acoustic trim based on geometric modeling and flow simulation for non-woven

In order to optimize the acoustic properties of a stacked fiber non-woven, the microstructure of the non-woven is modeled by a macroscopically homogeneous random system of straight cylinders (tubes). That is, the fibers are modeled by a spatially stationary random system of lines (Poisson line process), dilated by a sphere. Pressing the non-woven causes anisotropy. In our model, this anisotropy is described by a one parametric distribution of the direction of the fibers. In the present application, the anisotropy parameter has to be estimated from 2d reflected light microscopic images of microsections of the non-woven.
After fitting the model, the flow is computed in digitized realizations of the stochastic geometric model using the lattice Boltzmann method. Based on the flow resistivity, the formulas of Delany and Bazley predict the frequency-dependent acoustic absorption of the non-woven in the impedance tube.

Using the geometric model, the description of a non-woven with improved acoustic absorption properties is obtained in the following way: First, the fiber thicknesses, porosity and anisotropy of the fiber system are modified. Then the flow and acoustics simulations are performed in the new sample. These two steps are repeatedc for various sets of parameters. Finally, the set of parameters for the geometric model leading to the best acoustic absorption is chosen.
Keywords: random system of fibers, Poisson line process, flow resistivity, acoustic absorption, Lattice-Boltzmann method, non-woven
(21 pages, 2005)

73. V. Rutka, A. Wiegmann

Explicit Jump Immersed Interface Method for virtual material design of the effective elastic moduli of composite materials

Virtual material design is the microscopic variation of materials in the computer, followed by the numerical evaluation of the effect of this variation on the material's macroscopic properties. The goal of this procedure is an in some sense improved material. Here, we give examples regarding the dependence of the effective elastic moduli of a composite material on the geometry of the shape of an inclusion. A new approach on how to solve such interface problems avoids mesh generation and gives second order accurate results even in the vicinity of the interface.
The Explicit Jump Immersed Interface Method is a finite difference method for elliptic partial differential equations that works on an equidistant Cartesian grid in spite of non-grid aligned discontinuities in equation parameters and solution. Near discontinuities, the standard finite difference approximations are modified by adding correction terms that involve jumps in the function and its derivatives. This work derives the correction terms for two dimensional linear elasticity with piecewise constant coefficients, i. e. for composite materials. It demonstrates numerically convergence and approximation properties of the method.
Keywords: virtual material design, explicit jump immersed interface method, effective elastic moduli, composite materials
(22 pages, 2005)

74. T. Hanne

Eine Übersicht zum Scheduling von Baustellen

Im diesem Dokument werden Aspekte der formalen zeitlichen Planung bzw. des Scheduling für Bauprojekte anhand ausgewählter Literatur diskutiert. Auf allgemeine Aspekte des Scheduling soll dabei nicht eingegangen werden. Hierzu seien als Standard-Referenzen nur Brucker (2004) und Pinedo (1995) genannt. Zu allgemeinen Fragen des Projekt-Managements sei auf Kerzner (2003) verwiesen.
Im Abschnitt 1 werden einige Anforderungen und Besonderheiten der Planung von Baustellen diskutiert. Diese treten allerdings auch in zahlreichen anderen Bereichen der Produktionsplanung und des Projektmanagements auf. In Abschnitt 2 werden dann Aspekte zur Formalisierung von Scheduling-Problemen in der Bauwirtschaft diskutiert, insbesondere Ziele und zu berücksichtigende Restriktionen. Auf eine mathematische Formalisierung wird dabei allerdings verzichtet. Abschnitt 3 bietet eine Übersicht über Verfahren und grundlegende Techniken für die Berechnung von Schedules. In Abschnitt 4 wird ein Überblick über vorhandene Software, zum einen verbreitete Internationale Software, zum anderen deutschsprachige Branchenlösungen, gegeben. Anschließend werden Schlussfolgerungen gezogen und es erfolgt eine Auflistung der Literaturquellen.
Keywords: Projektplanung, Scheduling, Bauplanung, Bauindustrie
(32 pages, 2005)

75. J. Linn

The Folgar–Tucker Model as a Differential Algebraic System for Fiber Orientation Calculation

The Folgar–Tucker equation (FTE) is the model most frequently used for the prediction of fiber orientation (FO) in simulations of the injection molding process for short–fiber reinforced thermoplasts. In contrast to its widespread use in injection molding simulations, little is known about the mathematical properties of the FTE: an investigation of e. g. its phase space M_{FT} has been presented only recently [12]. The restriction of the dependent variable of the FTE to the set M_{FT} turns the FTE into a differential algebraic system (DAS), a fact which is commonly neglected when devising numerical schemes for the integration of the FTE. In this article we present some recent results on the problem of trace stability as well as some introductory material which complements our recent paper [12].
Keywords: fiber orientation, Folgar–Tucker model, invariants, algebraic constraints, phase space, trace stability
(15 pages, 2005)

76. M. Speckert, K. Dreßler, H. Mauch, A. Lion, G. J. Wierda

Simulation eines neuartigen Prüfsystems für Achserprobungen durch MKS-Modellierung einschließlich Regelung

Testing new suspensions based on real load data is performed on elaborate multi channel test rigs. Usually, wheel forces and moments measured during driving maneuvers are reproduced by the test rig. Because of the complicated interaction between test rig and suspension each new rig configuration has to prove its efficiency with respect to the requirements and the configuration might be subject to optimization.
This paper deals with mathematical and physical modeling of a new concept of a test rig which is based on two hexapods. The model contains the geometric configuration as well as the hydraulics and the controller. It is implemented as an ADAMS/Car template and can be combined with different suspension models to get a complete assembly representing the entire test rig. Using this model, all steps required for a real test run such as controller adaptation, drive file iteration and simulation can be performed. Geometric or hydraulic parameters can be modified easily to improve the setup and adapt the system to the suspension and the given load data.
The model supports and accompanies the introduction of the new rig concept and can be used to prepare real tests on a virtual basis. Using both a front and a rear suspension the approach is described and the potentials coming with the simulation are pointed out.
Keywords: virtual test rig, suspension testing, multibody simulation, modeling hexapod test rig, optimization of test rig configuration
(20 pages, 2005)
In deutscher Sprache; bereits erschienen in: VDI-Berichte Nr. 1900, VDI-Verlag GmbH Düsseldorf (2005), Seiten 227-246

77. K.-H. Küfer, M. Monz, A. Scherrer, P. Süss, F. Alonso, A. S. A. Sultan, Th. Bortfeld, D. Craft, Chr. Thieke

Multicriteria optimization in intensity modulated radiotherapy planning

Inverse treatment planning of intensity modulated radiothrapy is a multicriteria optimization problem: planners have to find optimal compromises between a sufficiently highdose intumor tissuethat garantuee a high tumor control, and, dangerous overdosing of critical structures, in order to avoid high normal tissue complcication problems.
The approach presented in this work demonstrates how to state a flexible generic multicriteria model of the IMRT planning problem and how to produce clinically highly relevant Pareto-solutions. The model is imbedded in a principal concept of Reverse Engineering, a general optimization paradigm for design problems. Relevant parts of the Pareto-set are approximated by using extreme compromises as cornerstone solutions, a concept that is always feasible if box constraints for objective funtions are available. A major practical drawback of generic multicriteria concepts trying to compute or approximate parts of the Pareto-set is the high computational effort. This problem can be overcome by exploitation of an inherent asymmetry of the IMRT planning problem and an adaptive approximation scheme for optimal solutions based on an adaptive clustering preprocessing technique. Finally, a coherent approach for calculating and selecting solutions in a real-timeinteractive decision-making process is presented. The paper is concluded with clinical examples and a discussion of ongoing research topics.
Keywords: multicriteria optimization, extreme solutions, real-time decision making, adaptive approximation schemes, clustering methods, IMRT planning, reverse engineering
(51 pages, 2005)

Status quo: July 2005